2016

Human central nervous system (CNS) ApoE isoforms are increased by age, differentially altered by amyloidosis, and relative amounts reversed in the CNS compared with plasma

Alaina T. Baker-Nigh
Washington University School of Medicine in St. Louis

Kwasi G. Mawuenyega
Washington University School of Medicine in St. Louis

James G. Bollinger
Washington University School of Medicine in St. Louis

Vitaliy Ovod
Washington University School of Medicine in St. Louis

Tom Kasten
Washington University School of Medicine in St. Louis

See next page for additional authors

THE JOURNAL OF BIOLOGICAL CHEMISTRY VOL. 291, NO. 53, pp. 27204–27218, December 30, 2016

Human Central Nervous System (CNS) ApoE Isoforms Are Increased by Age, Differentially Altered by Amyloidosis, and Relative Amounts Reversed in the CNS Compared with Plasma*

Received for publication, April 7, 2016, and in revised form, October 22, 2016 Published, JBC Papers in Press, October 28, 2016, DOI 10.1074/jbc.M116.721779

Alaina T. Baker-Nigh[‡], Kwasi G. Mawuenyega[‡], James G. Bollinger[‡], Vitaliy Ovod[‡], Tom Kasten[‡], Erin E. Franklin[§¶], Fan Liao[‡], Hong Jiang[‡], David Holtzman[‡¶‖], Nigel J. Cairns[‡§¶‖], John C. Morris[‡¶‖], and Randall J. Bateman[‡¶‖1]

From the Departments of [‡]Neurology and [§]Pathology and Immunology, [¶]Knight Alzheimer's Disease Research Center, and [‖]Hope Center for Neurological Disorders, Washington University, St. Louis, Missouri 63110

Edited by Paul Fraser

The risk of Alzheimer's disease (AD) is highly dependent on apolipoprotein-E (apoE) genotype. The reasons for apoE isoform-selective risk are uncertain; however, both the amounts and structure of human apoE isoforms have been hypothesized to lead to amyloidosis increasing the risk for AD. To address the hypothesis that amounts of apoE isoforms are different in the human CNS, we developed a novel isoform-specific method to accurately quantify apoE isoforms in clinically relevant samples. The method utilizes an antibody-free enrichment step and isotope-labeled physiologically relevant lipoprotein particle standards produced by immortalized astrocytes. We applied this method to a cohort of well characterized clinical samples and observed the following findings. The apoE isoform amounts are not different in cerebrospinal fluid (CSF) from young normal controls, suggesting that the amount of apoE isoforms is not the reason for risk of amyloidosis prior to the onset of advanced age. We did, however, observe an age-related increase in both apoE isoforms. In contrast to normal aging, the presence of amyloid increased apoE3, whereas apoE4 was unchanged or decreased. Importantly, for heterozygotes, the apoE4/apoE3 isoform ratio was increased in the CNS, although the reverse was true in the periphery. Finally, CSF apoE levels, but not plasma apoE levels, correlated with CSF β-amyloid levels. Collectively, these findings support the hypothesis that CNS and peripheral apoE are separate pools and differentially regulated. Furthermore, these results suggest that apoE mechanisms for the risk of amyloidosis and AD are related to an interaction between apoE, aging, and the amount of amyloid burden.

The largest risk factors for developing late-onset Alzheimer's disease (AD)[2] are advanced age and apolipoprotein-E (*APOE*) genotype. ApoE is a 34-kDa lipoprotein with 299 amino acid residues expressed primarily by astrocytes in the central nervous system (CNS) and by hepatocytes and macrophages in the periphery (CNS) (1). In humans, the *APOE* gene is polymorphic with three high frequency alleles, *APOE*-ϵ2, *APOE*-ϵ3, and *APOE*-ϵ4. The expressed allelic isoforms differ by single cystine-arginine replacements as follows: apoE2 (R112C and R158C), apoE3 (R112C), and apoE4 (2). These alleles are associated with differential AD risk, where *APOE*-ϵ2 is protective and *APOE*-ϵ4 increases risk in a dose-dependent manner (3- and 12-fold for heterozygotes and homozygotes, respectively) compared with the most prevalent *APOE*-ϵ3 allele (78% in the Caucasian American population (3, 4)). Taken together, variations in the *APOE* gene may account for at least 50% of the population-attributable risk in late-onset AD (5).

The role of apoE in AD pathogenesis has been attributed to numerous mechanisms based on both *in vitro* and *in vivo* observations (6). Briefly, apoE is a proteinaceous component of both plaques and tangles (7) that binds to and effects the deposition of β-amyloid (Aβ) in an isoform-dependent manner (8–10). ApoE4 exacerbates oligomerization (11), cortical plaque deposition (12), and intra-neuronal concentrations of Aβ (13–15). Furthermore, apoE isoform expression also impacts the clearance of Aβ (16), with the observed effects speculated to be dependent on each respective isoform's lipidation state and/or affinity for cognate receptors (17–19). Finally, there is also evidence of direct cleavage of the apoE4 isoform into toxic fragments within neurons (20) that are implicated in aberrant Tau phosphorylation (21). Taken together, it is clear that apoE isoform expression plays a central role in the modulation of AD pathology and that a better understanding of apoE pathophysiology is essential for apoE-directed drug development.

* This work was supported by National Institutes of Health Grants 5P50AG005681-31, R01NS065667, P01AG003991, and P01AG026276 and the Alzheimer's Drug Discovery Foundation. The authors declare that they have no conflicts of interest with the contents of this article. The content is solely the responsibility of the authors and does not necessarily represent the official views of the National Institutes of Health.

[1] To whom correspondence should be addressed: Washington University School of Medicine, 660 South Euclid Ave., Box 8111, St. Louis, MO 63110. Tel.: 314-362-3429; Fax: 314-362-2244; E-mail: batemanr@wustl.edu.

[2] The abbreviations used are: AD, Alzheimer's disease; Aβ, β-amyloid; ADNC, Alzheimer's disease neuropathological changes; apoE, apolipoprotein-E; CDR, clinical dementia rating; CSF, cerebrospinal fluid; ISTD, internal standard; SRM, serial reaction monitoring; PiB, Pittsburgh compound B; YNC, young normal control; ANOVA, analysis of variance; GFAP, glial fibrillar active protein.

To this end, multiple groups have attempted to establish whether isoform-dependent differences in the amount of apoE exist in the CNS. Astrocyte-derived apoE is a separate pool from liver-derived apoE in the periphery (22) and is found at concentrations of ~5–10 μg/ml in CSF and 50 μg/ml in plasma (23). Peripheral apoE measured in plasma has previously been shown to decrease with *APOE*-ϵ4 carrier status (23–26). In the CNS, ELISA-based methods for estimating the relative or absolute amounts of apoE allelic isoforms have yielded conflicting results, possibly due to isoform-specific antibody preference and inherent variability of the assay. For example, in human CSF, conflicting reports of increased apoE4 mole fraction (27), decreased apoE4 mole fraction (28), and an equal apoE4 mole fraction have been reported (29).

These inconsistent results indicate a need for validated simultaneous measures of apoE isoforms and robust quantitative methods with better precision and unbiased isoform specificity. One candidate technique is targeted mass spectrometry used in conjunction with stable isotope-labeled analytical standards (30). The decisive analytical advantages of this approach over the classically deployed immunoassays have led to its widespread application in clinical research laboratories. Previous efforts to use targeted proteomics to characterize allelic isoforms of apoE were based on isoform-specific tryptic peptides and typically relied on either isotope-labeled synthetic peptides (31) or recombinant proteins (32) as analytical standards. Studies that utilize synthetic peptide standards are unlikely to yield true absolute measurements due to their inability to control for variation introduced during the enrichment and proteolytic digestion steps of sample processing (both of which may introduce isoform-specific biases). Similarly, methods utilizing purified recombinant protein standards may also be insufficient. The behavior of lipidated apoE during purification differs distinctly from the purified non-lipidated protein (33). In an effort to address the shortcomings of these methods, we developed a targeted proteomics method that is both antibody-independent and based on a set of physiologically relevant human apoE3 and apoE4 stable isotope-labeled lipoprotein standards produced in mouse immortalized astrocytes. After initial assay validation, we applied this novel technique to a set of well characterized clinical samples in an effort to compare apoE isoform amounts without assay bias. We selected a wide range of samples from plasma, CSF, and brain with a range of ages and amount of amyloidosis to better understand the relationship between apoE isoform expression in the CNS and periphery within the context of increasing age and amyloid burden.

Results

Accuracy of Total and Isoform-specific ApoE Measures—After generation of the stable isotope-labeled apoE3 and apoE4 standards in independent cultures of immortalized astrocytes, we performed cross-titration experiments to ensure that the final internal standard mix contained equal amounts of apoE3 and apoE4. We determined that an apoE3/apoE4 ratio of 2.54:1 of labeled astrocyte-derived media stocks provided an equimolar mix of these isoforms, and we used this ratio to make the internal standard mix for all subsequent analyses (see Fig. 1*C*.)

To validate the accuracy of our stable isotope absolute quantitation using lipoprotein particle internal standards, we examined the consistency of our results across isoform-specific and four common peptides (reflecting total apoE). The common peptides in CSF were very strongly correlated to one another and to the isoform-specific peptide total (E3 in *APOE*-ϵ3/ϵ3, E4 in *APOE*-ϵ4/ϵ4, and sum of E3 and E4 in *APOE*-ϵ3/ϵ4 participants), with coefficients of correlation within participants of 0.95 or greater ($p < 0.0001$) and a slope of 1.025 for the common peptide average *versus* the isoform-specific sum (Table 1). For brain samples with quantitative measures of apoE isoforms (excluding *APOE*-ϵ2 carriers), isoform and common measures of total apoE were strongly correlated ($R = 0.93$; $p < 0.0001$) with a slope of 1.14. Similar results are obtained when the results are analyzed by apoE genotype (Fig. 1*D*).

Calibration curves for each peptide were constructed (data not shown), and all measurements reported fell within the linear portions of these curves. The lowest point on each calibration curve is reported as each peptide's lower limit (Table 2).

Measurement of plasma apoE by MS and ELISA exhibited a very strong correlation (Pearson's $R = 0.80$, $p < 0.0001$ for common peptides *versus* ELISA and $R = 0.86$, $p < 0.0001$ for isoform-specific peptides *versus* ELISA). MS and ELISA measures also demonstrated similar trends of decreasing total apoE with increasing apoE4 copy number, as has been widely reported previously (Fig. 2).

Absolute Amount of ApoE3 and ApoE4 Isoforms in CSF, Frontal Cortex, and Plasma—To determine whether the differential risk for AD by *APOE* genotype could be due to the apoE protein amount in the CNS, we examined apoE3 and apoE4 isoform amounts in CSF and brain from heterozygote carriers.

Higher apoE4 compared with apoE3 was observed in CSF and brain of nearly all *APOE*-ϵ3/ϵ4 individuals examined, whereas plasma from heterozygotes showed the opposite relationship (Fig. 3*A*). Student's *t* tests showed a higher mole fraction of apoE4 in heterozygote CSF, which reached statistical significance in this cohort, 53.0% apoE4 ($t(6) = 2.5$, $p < 0.05$) in YNCs, and 55.6% apoE4 ($t(34) = 17.8$, $p < 0.0001$) in the older cohort. Similarly, 56% apoE4 was observed in frontal cortex samples from heterozygotes $t(16) = 6.8$, $p < 0.0001$. For plasma within the same CSF subjects, the ratio reversed such that 70.7% of apoE was apoE3, $t(17) = 16.6$, $p < 0.0001$.

CSF and plasma apoE4/apoE3 isoform ratios were negatively correlated between paired plasma and CSF samples. A significant negative correlation (Pearson's $R = -0.47$, $R^2 = 0.022$, p (two-tailed) $= 0.047$) was observed between apoE4/apoE3 ratios from *APOE*-ϵ3/ϵ4 participants where both CSF and plasma were measured (Fig. 3*B*). In contrast, no significant correlations were found for total apoE, apoE3, and apoE4 amounts between plasma and CSF. These findings suggest opposite metabolism of apoE4 and apoE3 between the CNS and periphery.

Age-associated Increase in apoE—We assessed apoE isoform amounts in CSF across the adult life span. Comparing the means between age groups with age 60 as the cutoff, increasing age was correlated with a 39% increase in total apoE as measured by the four common peptides, 34% increase in gene dose-normalized apoE3 amount and 50% increase apoE4 amount.

ANOVA of gene dose-normalized amounts of total, apoE3, and apoE4 by age group was highly significant ($F(5,240) = 6.7$, $p < 0.0001$). Each comparison between age groups was individually significant within the analysis: total apoE $p = 0.006$, apoE3 $p = 0.04$, and apoE4 $p = 0.02$ (adjusted p values for multiple comparisons reported). Furthermore, linear regression of gene dose-normalized total apoE, apoE3, and apoE4 amounts revealed significant increases with age as follows: total (com-

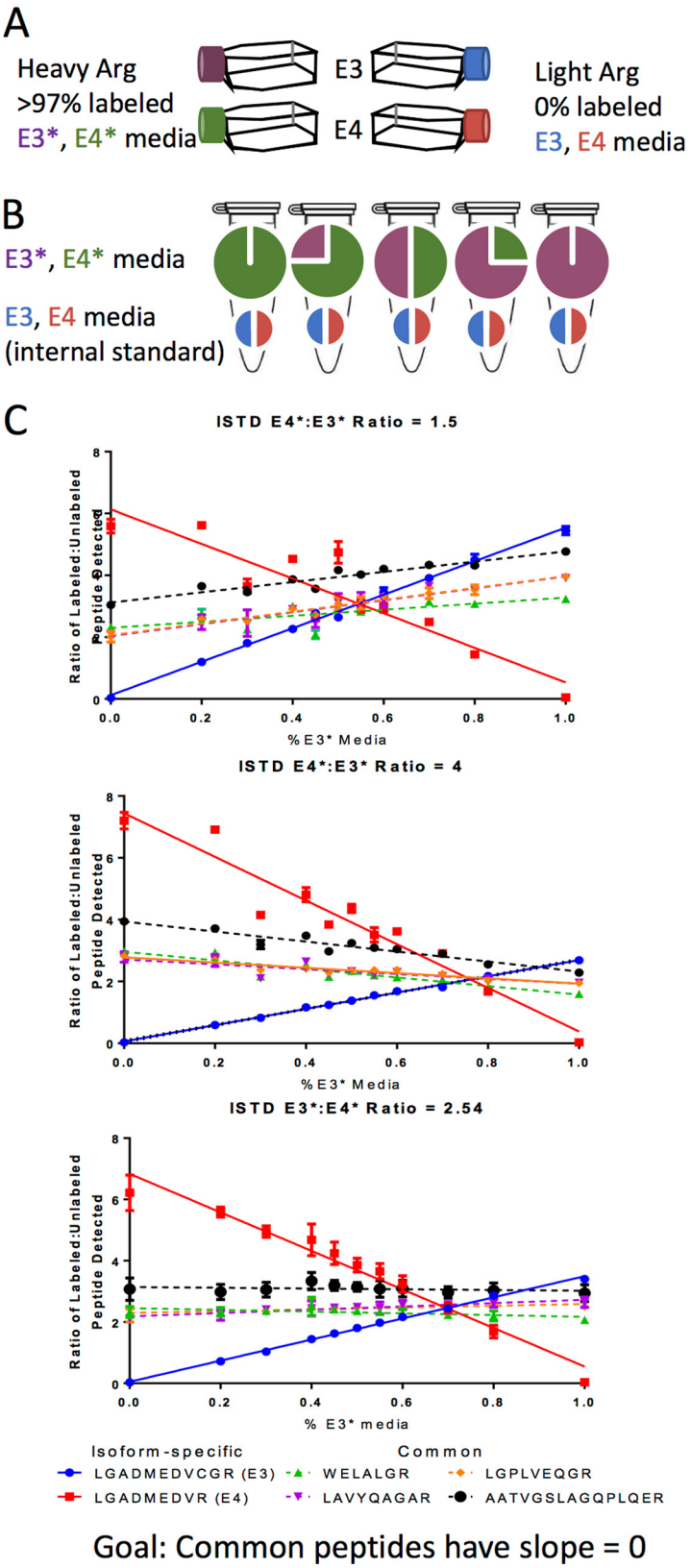

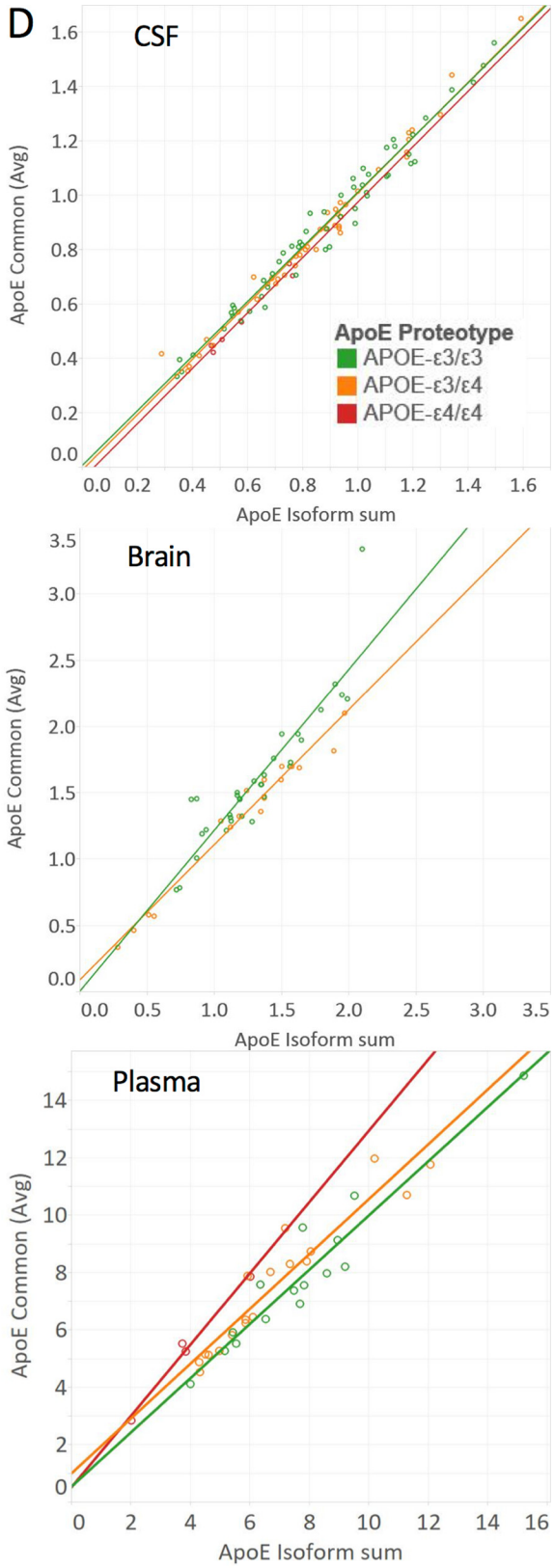

TABLE 1

Correlation of total apoE by common peptide and total apoE by summed isoform-specific peptide measures in human CSF

When plotted against the isoform-specific quantitation of total apoE in CSF samples, four common peptides demonstrated a high correlation within participants, with slopes near 1 and R^2 exceeding 0.93.

Peptide (*vs.* isoform sum)	Slope	R^2	Standard error	Significance, *p* value
AATVGSLAGQPLQER	1.024	0.933	0.078	<0.0001
LAVYQAGAR	1.001	0.962	0.057	<0.0001
LGPLVEQGR	1.045	0.965	0.057	<0.0001
WELALGR	1.015	0.960	0.059	<0.0001
Common-average	1.025	0.976	0.045	<0.0001

mon) apoE = 0.0058·age + 0.47, R^2 = 0.11, p = 0.0006; apoE3 amount = 0.0048·age + 0.51, R^2 = 0.87, p = 0.0035; apoE4 amount = 0.0070·age + 0.44, R^2 = 0.14, p = 0.0087, approximating an 8% increase in apoE amount per decade of life (Fig. 4). Similar linear trends were observed when data were restricted to β-amyloid-negative participants, although the trend for apoE4 did not reach significance because the majority of apoE4 carriers are β-amyloid-positive (37 *versus* 7 β-amyloid-negative in the older cohort and 9 in the YNC cohort).

To confirm the findings in YNC samples, which were initially processed separately from older CSF, a subset of YNC and older subject samples was reprocessed and analyzed simultaneously, and the results confirmed the effects and their magnitude.

β-Amyloidosis and Genotype Effects on ApoE Amount—To determine the effect of amyloidosis on apoE variant protein levels, gene dose-normalized variant amounts and total apoE were compared in those with and without amyloidosis. The strongest effect was observed in the CSF from β-amyloid-positive older participants. A decreasing amount of apoE was observed with *APOE*-ϵ4 carrier status (*APOE*-ϵ3/ϵ3 > *APOE*-ϵ3/ϵ4 > *APOE*-ϵ4/ϵ4) for total apoE (average common peptides; $F(2,40) = 1.4$, p = 0.0019; Fig. 5*C, bottom panel*), with mean(S.D.) apoE amounts of 1.06(0.20) > 0.90(0.26) > 0.53(0.12) normalized units. Similar independent decreases were observed for apoE3 (*APOE*-ϵ3/ϵ3 > *APOE*-ϵ3/ϵ4; mean(S.D.) = 0.52(0.10) > 0.40(0.11) normalized units; p = 0.0025) and apoE4 variants (*APOE*-ϵ3/ϵ4 > *APOE*-ϵ4/ϵ4; mean(S.D.) = 0.50(0.13) > 0.29(0.06); p = 0.0050; Fig. 5*C, top* and *middle panels*). A decrease in brain apoE3 in APOE-ϵ4 carriers was observed (*APOE*-ϵ3/ϵ3 > *APOE*-ϵ3/ϵ4; mean(S.D.) = 0.66(0.18) > 0.52(0.21); p = 0.02), but the same trend toward a decrease in total apoE in brain did not reach statistical significance (*APOE*-ϵ3/ϵ3 > *APOE*-ϵ3/ϵ4; mean(S.D.) = 1.59(0.49) > 1.31(0.52); p = 0.07; Fig. 5*D*). In the YNC cohort, older β-amyloid-negative cohort and plasma samples, neither variant nor total CSF apoE amounts (measured by average of the common peptides), differed by genotype when compared across groups (Fig. 5, *A, B, D,* and *E*). However, a trend toward a decrease with *APOE*-ϵ4 carrier status was confirmed in plasma when total apoE represented by the sum of the variant-specific peptide measures was performed (*APOE*-ϵ3/ϵ3 > *APOE*-ϵ3/ϵ4 > *APOE*-ϵ4/ϵ4; mean(S.D.) = 7.70(2.64) > 6.82(2.35) > 3.91(1.64); $F(2,34) = 3.9$, p = 0.03), although the effect failed to reach significance when the average common peptides were compared across genotypes (p = 0.21).

Of interest, frontal cortex from *APOE*-ϵ3/ϵ3 and *APOE*-ϵ3/ϵ4 participants contained a 50% higher concentration of apoE than CSF from the older cohort (Fig. 5, *B–D*). Plasma apoE concentration was ~10-fold higher than CSF (Fig. 5, *B, C,* and *E*).

To assess the effect of β-amyloidosis on total apoE and on apoE3 and apoE4 variants, a comparison was made by β-amyloid status (Fig. 6). *APOE*-ϵ3/ϵ3 participants, in particular, exhibited significant increases in total apoE and apoE3 amounts such that YNC < β-amyloid− < β-amyloid+. Within *APOE*-ϵ3/ϵ3 individuals, ANOVA demonstrated a significant difference in CSF apoE3 amount ($F(2,51) = 4.3$, p = 0.019), as well as total apoE ($F(2,51) = 5.9$, p = 0.0049). Post hoc comparisons showed that only the difference between YNC and amyloid+ groups reached statistical significance (p = 0.014 for apoE3 amount, p = 0.0034 for total apoE). A trend toward an increase in apoE3 amount with amyloidosis in the older *APOE*-ϵ3/ϵ3 cohort did not reach significance (p = 0.20 for apoE3 amount and p = 0.20 for total apoE). Within *APOE*-ϵ3/ϵ4 individuals, a similar result was seen for apoE4 amount ($F(2,39) = 4.2$, p = 0.023), with post hoc significance between YNC and amyloid+ groups (p = 0.021) and a trend for an increase between YNCs and amyloid− (p = 0.066). No difference was observed in apoE4 amount with amyloidosis in the older *APOE*-ϵ3/ϵ4 cohort (p = 0.99 for apoE3 amount, p = 0.99 for apoE4 amount, and p > 0.99 for total apoE). Within *APOE*-ϵ4/ϵ4 individuals, no differences were observed in apoE4 or total amounts between YNC and β-amyloid+ groups.

FIGURE 1. **Demonstration of molar equivalence of apoE3 and apoE4 in internal standard (heavy Arg media) and external standard (CSF titration curve).** *A*, lipoprotein particle standard production. Immortalized murine astrocytes expressing transgenic human *APOE*-ϵ3 or *APOE*-ϵ4 were incubated in stable isotope labeling media supplemented with light arginine (unlabeled) or heavy L-[U-$^{13}C_6$,$^{15}N_4$]arginine (labeled). Culture media were collected with no label (*E3* and *E4*) or at very high (>95%) label incorporation (*E3** and *E4**). *B*, lipoprotein particle cross-titration. To estimate the concentration of E3* media relative to E4* media, inverted dilution curves of E3*(decreasing) and E4*(increasing) media were added to a consistent volume of unlabeled E3/E4 media. Selected peptides were detected in a linear fashion by LC/SRM across the volumes used. *C*, lipoprotein particle molar equilibration. Although the titration proportions were held constant as shown in *B*, the actual volume of E4* media was adjusted to identify the E4*/E3* ratio where common peptides were detected equally along the cross-titration curve. At ratios of 1.5 (*C, top panel*) and 4 (*C, middle panel*) E4*/E3* media by volume, common peptides had positive and negative slopes, respectively, demonstrating different molar ratios. Based on these results, apoE molar equivalence was determined to be 2.54 times more concentrated in E3* than in E4* media (*C, bottom panel*). A dilution curve using 2.54:1 ratio was tested, and fit lines were found to have an average slope of 0.11 across four common peptides, indicating that the two standards were in molar equivalence. This equilibrated media ratio (note horizontal apoE amounts in mixing titration experiment) was used to incorporate isoform-equilibrated E3* and E4* internal standards in all samples. Similar cross-titration experiments were carried out using human *APOE*-ϵ3 and *APOE*-ϵ4 homozygote CSF (unlabeled, using molar equivalent E3*/E4* internal standards) to equilibrate standard curves used in absolute quantitation of isoforms (data not shown). *D*, correlation of total and isoform-specific apoE measures. Independent measures of CSF apoE common peptides (averaged for four peptides monitored) were consistent with the sum of isoform-specific peptides, producing a slope close to 1 (m = 1.025) by linear regression and a significant correlation (R^2 = 0.976, p < 0.0001). For brain samples from participants excluding *APOE*-ϵ2 carriers (isoform not monitored), the isoform and total apoE measures were slightly less precisely correlated (R^2 = 0.859, standard error = 0.195, p < 0.0001, with a slope of 1.14) but still approximated equivalent measures. Similarly, the correlation was also significant for plasma samples (R^2 = 0.898, standard error = 0.805, p < 0.0001, with a slope of 0.902).

TABLE 2

SRM data collection parameters

LLOQ's are reported as the mean (standard deviation) of the peak area ratio from the lowest non-zero point of each peptide's dilution curve of apoE3/apoE4 molar-equilibrated CSF plus E3*/E4* media lipoprotein internal standard (across three separate days of analysis).

Variant	Peptide	Precursor ion *m*/*z*	Product ion *m*/*z*	Collision energy	Peak area ratio LLOQ
Common	WELALGR	422.737	345.224 416.261 529.345 658.388	18	1.09 (0.05)
	WELALGR ($^{13}C_6$,$^{15}N_4$-R)	427.741	355.232 426.269 539.353 668.396	18	
E3/E4	LAVYQAGAR	474.767	665.336 764.404 835.442	19	1.07 (0.10)
	LAVYQAGAR ($^{13}C_6$,$^{15}N_4$-R)	479.771	675.344 774.413 845.450	20	
Common	LGPLVEQGR	484.780	588.309 701.394 798.446 855.468	20	1.12 (0.08)
	LGPLVEQGR ($^{13}C_6$,$^{15}N_4$-R)	489.784	598.318 711.402 808.455 865.476	20	
E4	LGADMEDVR	503.237	649.297 764.324 835.361 892.382	20	1.09 (0.06)
	LGADMEDVR ($^{13}C_6$,$^{15}N_4$-R)	508.241	659.305 774.332 845.369 902.391	21	
E2/E3	LGADMEDVcGR	611.763	735.309 866.349 981.376 1009.434	24	1.004 (0.10)
	LGADMEDVcGR ($^{13}C_6$,$^{15}N_4$-R)	616.767	745.317 876.357 991.384 1119.443	24	
Common	AATVGSLAGQPLQER	749.405	642.356 827.437 898.474 1155.611	29	0.70 (0.04)
	AATVGSLAGQPLQER ($^{13}C_6$,$^{15}N_4$-R)	754.409	652.365 837.445 908.482 1165.619	29	

Neuropathology Measures and Brain ApoE—To assess potential effects of mild Alzheimer's disease neuropathologic change (ADNC) in cognitively normal brain donors, particularly Aβ and Tau accumulation, comparisons were made between pathology measures and CNS apoE protein amounts. For brain samples, pathology measures in adjacent tissue (frontal neocortex) by genotype are reported in Table 3. ANOVA of pathology measures by apoE genotype demonstrated no significant relationships except for area fraction of β-amyloid immunohistochemistry (10D5 antibody); $F(3,42) = 3.8$, $p = 0.017$. Post hoc Tukey's analysis showed an increase in area fraction in *APOE*-ϵ3/ϵ4 compared with *APOE*-ϵ3/ϵ3 participants, $p = 0.041$. No correlational relationship was observed between apoE amounts (gene dose-normalized isoform-specific or total as the average of common peptides) and pathology, including Aβ area fraction and area fraction of phosphorylated Tau (PHF-1 antibody), nor with global pathology as assessed by Braak staging of neurofibrillary tangles (34), CERAD staging of neuritic plaques (35), or Thal Aβ staging (36). A positive correlation between apoE amounts and luminance of glial fibrillar active protein (GFAP), a marker of astrocytosis, was observed (total (common) apoE = 0.018·GFAP luminance, 1.2, $R^2 = 0.14$, $p = 0.011$).

For both CSF and plasma samples, individual measures of Aβ pathology amounts, namely PiB score and CSF Aβ 42:40 ratio, were not found to linearly correlate with apoE amounts. However, correlations between CSF (but not plasma) apoE amounts and CSF Aβ40 and Aβ42 amounts were robust (Fig. 7). For Aβ40 amount and CSF apoE3 isoform amount, the correlations were highly similar between β-amyloid-positive (Pearson's $R = 0.77$, $p < 0.0001$) and β-amyloid-negative participants ($R = 0.78$, $p < 0.0001$). This was also true for Aβ40 and apoE4 (β-amyloid-positive, $R = 0.84$, $p < 0.0001$; β-amyloid-negative, $R = 0.83$, $p < 0.05$) and total apoE amounts (β-amyloid-positive, $R = 0.81$, $p < 0.0001$; β-amyloid-negative, $R = 0.79$, $p < 0.0001$). For Aβ42 amount and apoE amount, the trends were less similar between β-amyloid status groups but still demonstrated significant correlations (apoE3 for β-amyloid-positive,

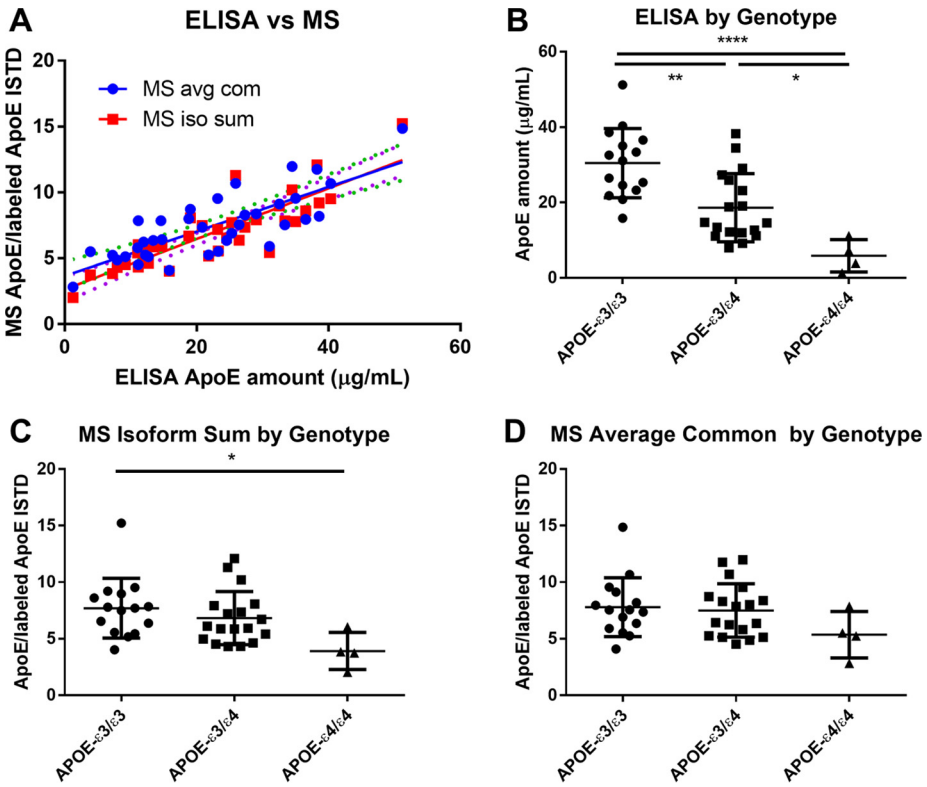

FIGURE 2. **Method comparison of apoE quantitation, ELISA *versus* MS (average common and isoform sum).** *A*, correlation of results. Total apoE from duplicate plasma samples including apoE3 and apoE4 carriers ($n = 15$ *APOE*-ε3/ε3, 18 *APOE*-ε3/ε4, and 4 *APOE*-ε4/ε4 participants) were analyzed by ELISA and MS. Whether apoE MS was calculated by the common peptides or isoform-specific peptides, a very strong correlation with ELISA was observed ($R = 0.80$, $p < 0.0001$ for average common MS *versus* ELISA, $R = 0.86$, $p < 0.0001$ for isoform sum MS *versus* ELISA). *B–D*, decreasing apoE with increasing *APOE*-ε4 copy number. ELISA analysis demonstrated a decrease in apoE amount with each additional *APOE*-ε4 allele, with each between-group sub-analysis reaching statistical significance: *APOE*-ε3/ε3 *versus APOE*-ε4/ε4 $p < 0.0001$, *APOE*-ε3/ε3 *versus APOE*-ε3/ε4 $p < 0.005$, *APOE*-ε3/ε4 *versus APOE*-ε4/ε4 $p < 0.05$ (*B*). In contrast, the mass spectrometry method did not show differences between *APOE*-ε3/ε3 *versus APOE*-ε3/ε4 in plasma and did not reach statistical significance between genotypes with MS measures for averaged common peptides (*D*); however, differences between *APOE*-ε3/ε3 and *APOE*-ε4/ε4 genotypes were significant, $p < 0.05$, when the comparison was based on isoform sum (*C*). In this figure and subsequent figures, "*apoE/labeled apoE ISTD*" as an axis label refers to the ratio of the endogenous analyte unlabeled apoE to the labeled apoE internal standard as measured by ion intensity of the area under the curve for the chromatographic peak, divided by starting volume of analyte (μl), and normalized to the standard curve.

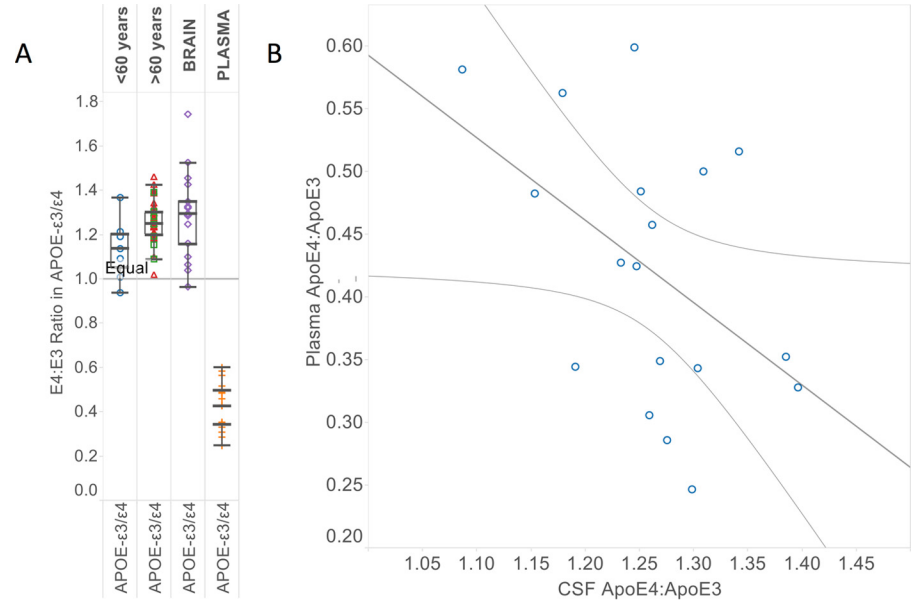

FIGURE 3. **ApoE4/apoE3 ratio and inverse relationship between blood apoE and CNS (CSF and brain) apoE.** *A*, isoform ratios. Student's *t* tests showed a higher ratio of apoE4/apoE3 in heterozygote CSF, which reached statistical significance in this cohor:1.14 ($t(6) = 2.5$, $p < 0.05$) in YNCs and 1.26 ($t(34) = 17.8$, $p < 0.0001$) in the older cohort. Similarly, a ratio of apoE4/apoE3 of 1.29 was observed in brain ($t(16) = 6.8$, $p < 0.0001$). For plasma from a subset of the same older CSF participants, a ratio of <1 indicates an inverse relationship where apoE4/apoE3 = 0.42 ($t(17) = 16.6$, $p < 0.0001$). *B*, inverse peripheral and CNS ratios. In plasma and CSF from heterozygote participants with both CSF and plasma analyzed, the apoE4/apoE3 ratios are inversely correlated; slope = −0.66, Pearson's $R = -0.47$, $R^2 = 0.022$, p (two-tailed) = 0.048.

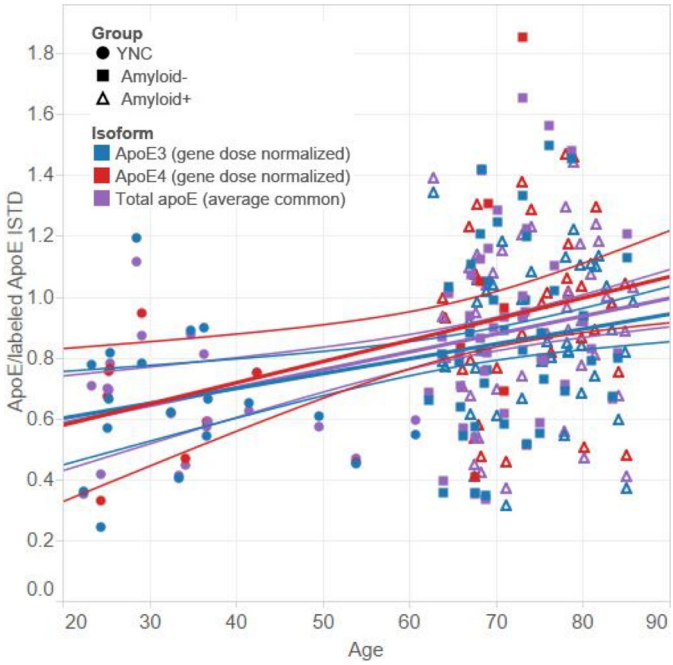

FIGURE 4. **ApoE increases with age.** A significant positive correlation was observed between aging and gene dose-normalized apoE3 ($R^2 = 0.092$, $p < 0.005$) and apoE4 isoforms ($R^2 = 0.142$, $p < 0.01$) as well as total apoE amounts in CSF ($R^2 = 0.117$, $p < 0.0005$). The effect was still observed when data were restricted to β-amyloid-negative and YNC participants (*solid markers*) in apoE3 ($R^2 = 0.124$, $p < 0.01$) and total apoE ($R^2 = 0.153$, $p < 0.005$), with a trend toward increase in apoE4 amount ($R^2 = 0.230$, $p = 0.060$). Biomarker-validated amyloid status was not available for YNC cases.

$R = 0.61$, $p < 0.0001$; apoE3 for β-amyloid-negative participants, $R = 0.67$, $p < 0.0001$; apoE4 for β-amyloid-positive, $R = 0.69$, $p < 0.0001$; total apoE for β-amyloid-positive, $R = 0.64$, $p < 0.0001$; total apoE for β-amyloid-negative participants, $R = 0.65$, $p < 0.0001$) with the exception of apoE4 for β-amyloid-negative participants ($p = 0.16$).

Discussion

We developed and utilized an apoE isoform-specific method that is antibody-free to more accurately quantify the amounts of apoE3 and apoE4 isoforms in CSF, brain, and plasma. The novel aspect of this method is its use of physiologically relevant stable isotope-labeled apoE lipoprotein particle standards. All standards (apoE3 and apoE4, stable isotope-labeled and -unlabeled) were produced in immortalized astrocytes and presumably mimic each isoform's native conformation *in vivo*. This approach enables both the standards and analytes to be subjected to the same manipulation (protein pulldown, digestion, alkylation, washes, etc.) prior to LC-MS analysis, which corrects for any isoform-specific bias that might be introduced during sample preparation. Furthermore, we employed an antibody-free affinity purification step that ensures all apoE detected (standards and analytes) consists of soluble lipoprotein particles with similar physiochemical properties, including the mass balance of apoE, cholesterol, and phospholipid as well as a lipoprotein particle size comparable with high density lipoprotein (33, 37). One notable difference is the lack of a cholesterol-ester core in the medium-derived apoE lipoprotein. This is consistent with the astrocyte-derived lipidated species that constitutes the major component of CNS apoE but differs from hepatocyte-derived apoE lipoprotein in the periphery.

As stated previously, ELISA-based methods for the characterization of apoE in the human CNS have yielded conflicting results. Although generally robust, immunoassays carry a not-insignificant risk of interferences and biases that could potentially introduce confounding factors to a study. The potential interferences include the high-dose hook effect, specificity shortcomings, autoantibodies, and anti-reagent antibodies (38). Furthermore, ELISA-based assays lack the ability to measure isoforms independently, detect truncations or fragments, and identify post-translational modifications. Finally, because the accuracy of an ELISA is entirely predicated by the standard with which it is calibrated, these assays lack the necessary concordance across platforms, which ultimately hinders comparisons between studies. Because of these and other limitations, LC-MS methodologies have emerged as a detection method capable of alleviating many of these inherent shortcomings. This work represents an extension of the previous development of LC-MS methods (31, 32) and directly addresses a potential source of bias (physiochemical differences between standard and analyte) in these assays.

We applied our antibody-free and isoform-specific LC-MS method to CSF and plasma samples from a cohort of APO-ϵ3/ϵ3, APO-ϵ3/ϵ4, and APO-ϵ4/ϵ4 study participants that spanned a spectrum of both age and amyloid burden. In addition, we applied the method to 41 well characterized post-mortem brain samples (as assessed by relevant biomarker measures). A few caveats of this study include the relatively low number of *APOE*-ϵ4/ϵ4 homozygote participants and the exclusion of *APOE*-ϵ2 carriers entirely. Both of these caveats are a reflection of the population prevalence of these apoE genotypes and their low frequency in the studied cohort, precluding meaningful interpretation of results. *APOE*-ϵ2 carriers were left out because of the very low prevalence in the population (~7%), and power analyses at the design phase of the study indicated very low probability of meaningful comparisons. Thus, we did not develop standards for apoE2 or measure apoE2 alleles. Our primary aims of the grant were specific for the apoE3 *versus* apoE4 comparison. Future studies may focus on this, but many hundreds of samples will be needed for the comparison. Similarly, another caveat to the reported analysis is that all *APOE*-ϵ4/ϵ4 participants in the older cohort are universally β-amyloid-positive. Additionally, our analyses of post-mortem brain tissues lacked *APOE*-ϵ4/ϵ4 participants due the exclusion of participants with existing AD neuropathology. Although both of these limitations are to be expected based on the well established amyloid and AD risk for *APOE*-ϵ4/ϵ4 individuals in this age range (40), they prevent a fully independent assessment of age and β-amyloidosis effects on apoE4 amount in homozygous carriers.

In contrast to previous studies (27, 41), this study observed no significant difference in apoE isoform expression in the CSF from the cohort of YNC. This important finding suggests that an isoform imbalance prior to the onset of advanced age is unlikely the reason for the elevated risk that *APOE*-ϵ4 carriers have for amyloidosis. We did observe, however, an age-related increase in apoE across all isoforms. Previous studies of this

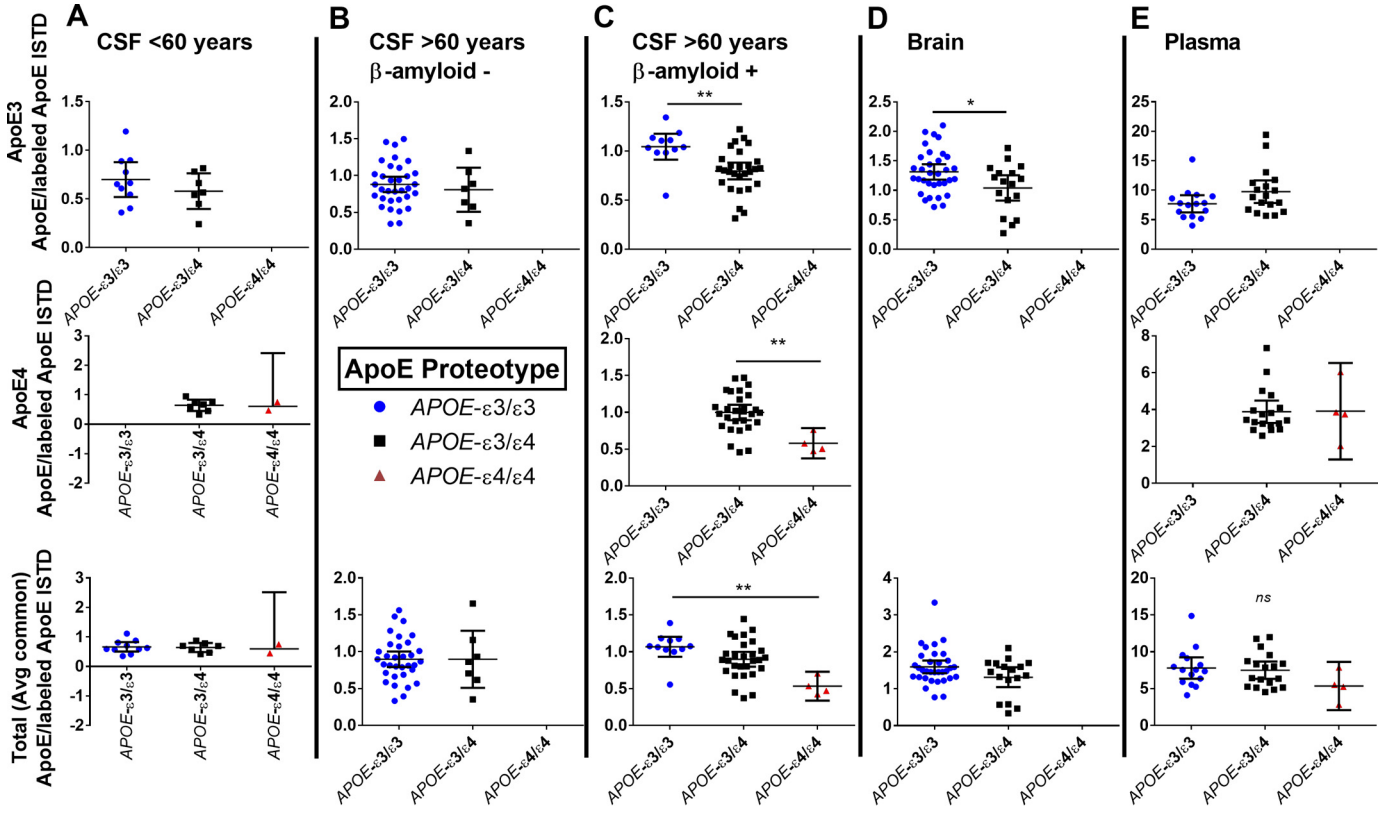

FIGURE 5. **ApoE isoform amounts are equal in young healthy CSF, but amyloidosis is associated with decreased apoE with increasing *APOE-ϵ4* copy number.** A decrease in apoE3, apoE4, and apoE total amount was associated with *APOE-ϵ4* carrier status such that *APOE-ϵ3/ϵ3* > *APOE-ϵ3/ϵ4* > *APOE-ϵ4/ϵ4* (*C*). This decrease was not observed in YNC participants (*A*), β-amyloid-negative older participants (*B*), or plasma (*E*), although a decrease in plasma total apoE was significant ($p < 0.05$, not shown) when total apoE was measured by isoform sum rather than average common peptides. A similar decrease was seen in apoE3 amount, but not significant in total apoE, in brain samples (*D*). Results for isoform amounts were normalized for gene dose for comparison across genotypes (see statistical methods). *Error bars*, 95% CI; *, $p < 0.05$; **, $p < 0.01$.

effect have yielded conflicting results. One study noted an age-dependent decline in APOE levels in the control population but an increase in the AD participants (42), although other studies observed an age-dependent increase in APOE3 across all participants (43, 44). This work is in agreement with the latter and nicely extends other previous work that noted an age-dependent up-regulation of cholesterol trafficking genes that coincided with the onset of cognitive impairment (44, 45). The notable exception to this trend in this study is in *APOE-ϵ4/ϵ4* participants, where apoE expression does not appear to increase as a function of age when combined with β-amyloidosis. This relationship should be further tested by evaluating both younger *APOE-ϵ4/ϵ4* individuals and older amyloid-negative *APOE-ϵ4/ϵ4* individuals. However, as mentioned above, the rarity of the latter group would make finding a suitable cohort for these analyses a significant challenge. All things considered, if increasing CNS apoE amount is a protective response to age and pathology, then the lack of response from *APOE-ϵ4* could potentially be a reason for the increased risk in AD. Alternatively, *APOE-ϵ4* may also selectively deposit in the CNS into amyloid plaques.

Also observed was an apoE isoform-dependent interaction with β-amyloidosis in the human CNS. In *APOE-ϵ3/ϵ3* participants, apoE increases with age and further increases with β-amyloidosis. Total apoE is elevated with increased age in *APOE-ϵ3/ϵ4* participants but does not further increase with β-amyloidosis. Furthermore, a decrease in gene dose-normalized apoE4 is seen with increasing *APOE-ϵ4* genotypes most distinctly in the β-amyloid-positive condition. It is notable that, in comparison with recent work quantitating apoE isoform amounts in the CNS by LC-MS with synthetic peptide standards (25), we observed increases in CSF apoE3 in amyloidosis and, in contrast, decreased CSF apoE4 in amyloidosis. The latter of which was not apparent in the study normalized with synthetic peptide standards. This differential response of apoE3 and apoE4 amounts in response to amyloidosis may reflect a part of the mechanism that underlies AD risk. However, a timeline for these changes relative to amyloid aggregation that is properly controlled for the age-related increase in apoE remains to be elucidated. Whether or not *APOE-ϵ4/ϵ4* participants would be expected to demonstrate an age-related increase in apoE in the absence of β-amyloid cannot be determined from the current dataset due to the lack of older β-amyloid-negative *APOE-ϵ4* homozygous participants. Again, obtaining CSF from *APOE-ϵ4/ϵ4* individuals who are cognitively robust in later life, particularly if they can be demonstrated to have low levels of Aβ accumulation, would greatly enhance the interpretation of the stated observations.

In post-mortem brain tissue samples, cases with a modest level of ADNC, apoE amount was increased (~50%), approximately the same order of magnitude as observed in CSF. Notably, the age effect observed in CSF may also contribute to this

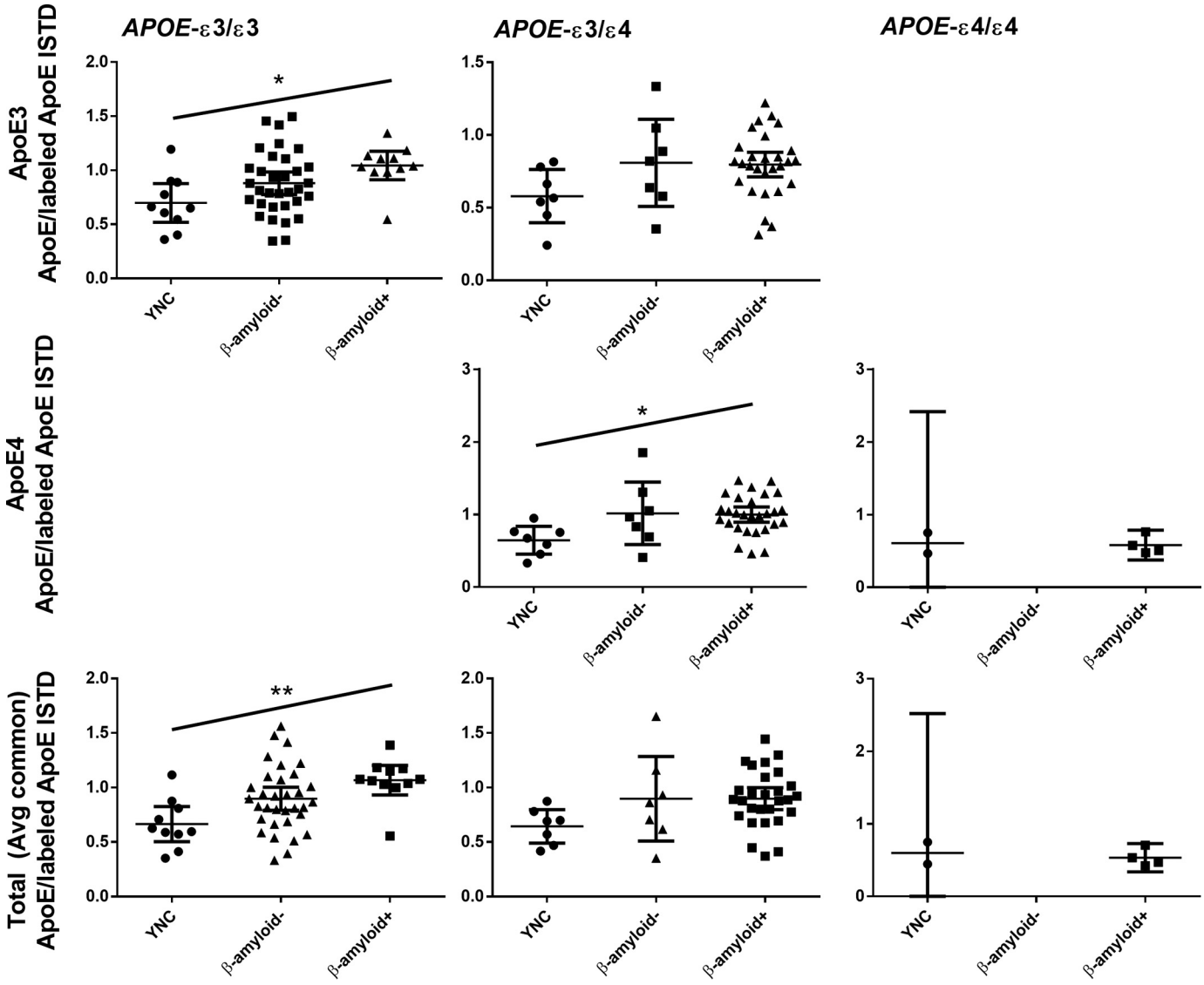

FIGURE 6. **Age-dependent increase in apoE for *APOE*-ϵ3/ϵ3 participants.** Comparing dose-normalized isoforms and total apoE within genotypes, a trend emerged for increasing apoE amounts where YNC < β-amyloid− < β-amyloid+. For the *APOE*-ϵ3/ϵ3 genotype, an increased range of apoE levels was evident with aging, with β-amyloid+ individuals falling typically into the upper half of the range. ANOVA demonstrated a significant difference in CSF apoE3 amount ($F(2,51) = 4.3$, $p = 0.019$), as well as total apoE ($F(2,51) = 5.9$, $p = 0.0049$). Post hoc comparisons showed that only the difference between YNC and amyloid+ groups reached statistical significance ($p = 0.014$ for apoE3 amount and $p = 0.0034$ for total apoE). A trend toward increase in apoE3 amount with amyloidosis in the older *APOE*-ϵ3/ϵ3 cohort did not reach significance ($p = 0.20$ for apoE3 amount and $p = 0.20$ for total apoE). Between-group differences only reached significance for *APOE*-ϵ3/ϵ4 participants in apoE4 isoform amount, again between young and β-amyloid+ groups. ANOVA showed increased apoE4 amount ($F(2,39) = 4.2$, $p = 0.023$), with post hoc significance between YNC and amyloid+ groups ($p = 0.021$) and a trend for increase between YNCs and amyloid− ($p = 0.066$). However, the trend toward higher apoE levels with β-amyloid presence was not observed in the older *APOE*-ϵ3/ϵ4 cohort; no difference was observed in apoE4 amount with amyloidosis ($p = 0.99$ for apoE3 amount, $p = 0.99$ for apoE4 amount, and $p > 0.99$ for total apoE). *APOE*-ϵ4/ϵ4 YNC and β-amyloid+ participants did not demonstrate a difference in APOE levels by Student's *t* test ($p = 0.99$ for apoE3 amount, $p = 0.99$ for apoE4 amount, and $p > 0.99$ for total apoE), although no older β-amyloid-negative participants with this genotype were available for comparison.

TABLE 3

Pathology quantitation of frontal cortex adjacent brain tissue

Values are reported as mean (95% confidence intervals) except for All brain, which is reported as mean (range). AF indicates area fraction of Aβ plaques/phosphorylated Tau in frontal neocortex (range: 0 to 1; 1 is 100% of cortex); GL indicates gray level, mean luminance of frontal neocortex (range: 0 to 256; 0 is most intense staining). Thal Aβ stage indicates global Aβ deposition staging protocol (range: 0, 1 to 5; 5 is most severe); Braak NFT stage indicates global NFT staging protocol (range: 0, 1 to 6; 6 is most severe). CERAD NP stage indicates neuritic plaque deposition staging (range: 0, 1 to 3; 3 is most severe).

ApoE genotype	Aβ (10D5)-AF	pTau (PHF1)-AF	Astrocytosis (GFAP)-GL	Thal Aβ stage	Braak NFT stage	CERAD NP stage	Brain weight
All brain	0.0399 (0.0000–0.1870)	0.0019 (0.0000–0.0405)	147.8 (124–168)	2.3 (0–5)	2.6 (1–6)	1.1 (0–4)	1208.0 (960–1450) [g]
APOE-ϵ3/ϵ3 $n = 31$	0.0275 (0.0136–0.0414)	0.0018 (−0.0013–0.0380)	148.9 (144.2–153.7)	2.0 (1.4–2.6)	2.6 (2.1–3.1)	1.2 (0.6–1.7)	1212.1 (1164–1260)
APOE-ϵ3/ϵ4 $n = 10$	0.0736 (0.0267–0.1204)	0.0041 (−0.0050–0.0133)	146.2 (139.1–153.3)	2.8 (1.9–3.7)	3.1 (2.2–4.0)	1.0 (0.3–1.8)	1226.0 (1157–1295)

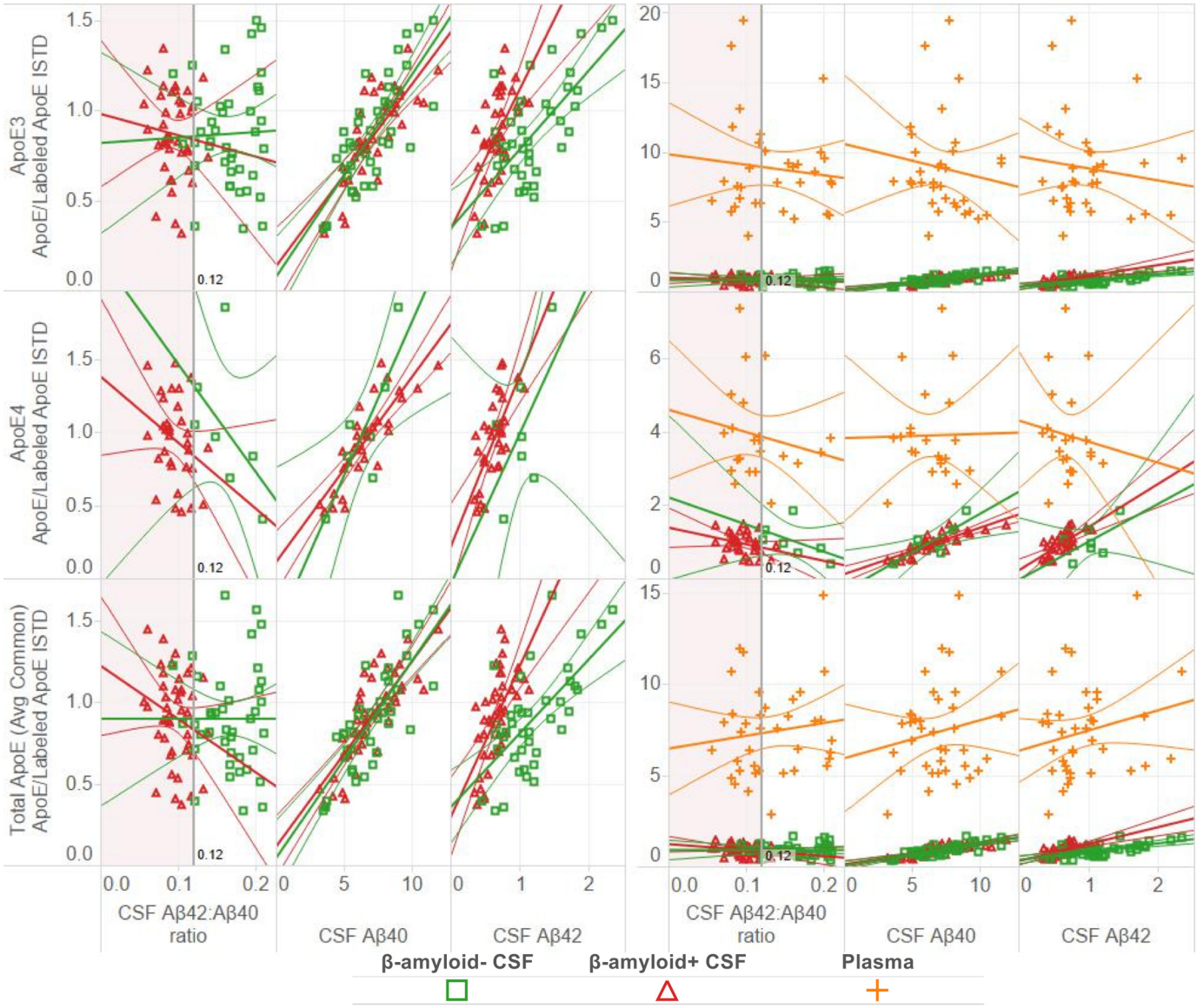

FIGURE 7. **CSF apoE amount, but not plasma apoE amount, is correlated to CSF β-amyloid amount.** Although no correlation was observed between CSF apoE amount and Aβ42/Aβ40 ratio, apoE and isoform amounts were positively correlated with Aβ40 and Aβ42 absolute amounts (*left panel*). All correlations were highly significant ($p < 0.0001$) except apoE4 amount for amyloid-negative carriers, where the relationship with Aβ40 reached significance ($p = 0.022$) and Aβ42 did not ($p = 0.58$). Although the relationship between Aβ40 and apoE is highly similar between β-amyloid− and β-amyloid+ groups, the slopes of the correlations differ by group for Aβ42 such that apoE amount rises more with increasing Aβ42 among β-amyloid+ participants than among β-amyloid− participants. Plasma apoE amount was not significantly correlated with CSF Aβ42/Aβ40 ratio, Aβ40 amount, or Aβ42 amount (*right panel*). *Panel tinting* demarcates categorically β-amyloid+ where Aβ42/Aβ40 < 0.12.

difference, as the post-mortem cases were older on average than the older cohort of CSF study participants. Also similarly to CSF, in *APOE*-ϵ3/ϵ4 heterozygous cases, brain exhibits a slightly increased apoE4/apoE3 ratio (30%). Thus, where ADNC is modest, CSF absolute quantitation of apoE isoform amounts provides a good readout of brain tissue apoE levels, with the relevant caveat that post-mortem brain tissue may be affected by additional factors such as agonal state and post-mortem interval. When compared with adjacent or global measures of pathology, no relationships with apoE levels were observed except for a positive correlation with a marker of astrocytes (GFAP). GFAP has many roles in astrocyte behavior, including motility, proliferation, maintaining the blood-brain barrier, and injury response, and it is commonly used as a marker of astrocytosis in neurodegenerative diseases (46). Because CNS apoE is primarily astrocytic in origin (47), a relationship between astrocyte prevalence and apoE amount is not surprising.

Furthermore, a robust imbalance in apoE isoform distribution in the *APOE*-ϵ3/ϵ4 heterozygote participants was observed in this work. This imbalance was reversed between the periphery (apoE3 > apoE4) and the CNS (apoE4 > apoE3). Previous studies have noted a reduced apoE4 mole fraction in the periphery (27, 41, 48–50). This imbalance has traditionally been attributed to a difference in the distribution of each isoform among the different sets of lipoprotein classes (48) that results in an enhanced clearance of apoE4-containing lipoprotein particles (49). Specifically, it is believed that peripheral apoE4

binds preferentially to larger lower density lipoproteins, whereas peripheral apoE3 prefers the smaller cholesterol-rich lipoproteins. The resulting increase in apoE to particle ratio in the lower density apoE4-containing particles results in a more rapid uptake of these lipoprotein particles by effectively enhancing their affinity for the cognate receptor (50). In the CNS (both brain and CSF), however, a reversal of this imbalance was observed by this study. Although this finding was also reported in previous work (27), it is in stark contrast to another study that reported a reduced apoE4 mole fraction in the CNS comparable with the imbalance observed in the periphery (51). Together, these observations suggest different mechanisms of clearance for apoE-containing particles in the CNS than the periphery.

Finally, this study suggests that CSF apoE levels, but not plasma apoE levels, correlate with Aβ in CSF. The association between apoE and Aβ is well documented, and several potential mechanisms for this association have been hypothesized (6, 52). Some studies have observed that apoE receptors play key roles in Aβ production. Other studies have pointed to an isoform-dependent enhancement of Aβ aggregation or impairment of Aβ clearance. Independent of the mechanism for this correlation, the current findings also support the hypothesis that central and peripheral apoE are separate pools and are subjected to different metabolism. However, the observed negative correlation between CSF and plasma apoE4/apoE3 ratios leaves open the possibility of a shared regulatory mechanism with opposite physiologic effects in each respective compartment. These results, along with the functional understanding of apoE trafficking in the CNS (where astrocytes and microglia package lipids for local neuronal use) *versus* periphery (where lipoprotein particles are released from the liver to the blood for relatively long-distance lipid transport), indicate that using plasma apoE as a biomarker readout of CNS apoE amounts is unlikely to be a useful strategy. Furthermore, the divergent ratios observed between sample types reduce the likelihood that these differences are due to inherent bias in the assay.

Taken together, the results from this study highlight the importance of focusing on CNS-derived studies when evaluating an apoE isoform-dependent risk for amyloidosis and AD. Furthermore, they suggest that assessment of this risk should properly control for the possible confounding factors of advanced age and amyloid burden. Further clarity into isoform-dependent mechanisms holds the potential for improved therapeutics for both the prevention and treatment of AD.

Experimental Procedures

CSF, Brain, and Plasma—Human studies took place at the Washington University School of Medicine in St. Louis and were approved by the Washington University Human Studies Committee and the General Clinical Research Center Advisory Committee. All participants gave informed written consent.

Human CSF was collected via lumbar catheter from 20 healthy young cognitively normal control (YNC: 22–60 years, average 34.5 ± 10.3 years, 8 female, 12 male) volunteers with a familial history (parent or grandparent) of AD. Additionally, 83 older participants (40 female, 43 male) with mild AD dementia (clinical dementia rating; CDR = 0.5–1) and age-matched controls were recruited in Aβ metabolism studies (53). Amyloidosis in this cohort was determined by Positron Emission Tomography imaging with [^{11}C]Pittsburgh compound B (PiB) performed within 3 years of study date, where an MCBP score higher than 0.18 was considered β-amyloid+ (54–56). For participants without PiB imaging, LC/MS measurement of CSF Aβ isoforms, specifically a concentration ratio of Aβ42/Aβ40 lower than 0.12, was used to identify β-amyloid+ individuals (54, 55). These criteria resulted in 40 older β-amyloid-negative (62–85 years, average 71.8 ± 5.9 years) and 43 β-amyloid-positive individuals (62–85 years, average 74.8 ± 6.7 years). *APOE* genotype was determined by PCR by the Genetics Core in of the Washington University Knight Alzheimer Disease Research Center, and genotype was confirmed *versus* prototype by MS isoform-specific peptide detection for all cases.

TABLE 4
Number of participants are by *APOE* genotype
Numbers and mean age (standard deviation) of CSF, plasma, and brain samples are presented by experimental group and *APOE* genotype. Amyloid status was not available for YNC participants.

Participants	*APOE*-ε3/ε3	*APOE*-ε3/ε4	*APOE*-ε4/ε4	Total
YNC CSF	10	7	2	19
	36.0 (11.3)	31.4 (10.78)	38.4 (5.85)	34.6 (10.60)
Amyloid+ CSF	11	28	4	43
	75.3 (7.57)	75.2 (6.44)	70.6 (6.44)	74.8 (6.72)
Amyloid− CSF	33	7	0	40
	72.3 (6.25)	69.2 (2.54)		71.8 (5.93)
Plasma	15	18	4	37
	73.5 (6.23)	73.5 (6.92)	70.6 (6.44)	73.1 (6.46)
Brain	31	10	0	41
	85.9 (9.55)	84.1 (10.42)		85.5 (9.67)
Total	100	70	10	180

Human plasma was retrieved from blood collected at the time of initial lumbar puncture in CSF studies and stored at −80 °C until use. Plasma from a subset of the older cohort of participants (n = 37; 23 females and 14 males) was analyzed for this study.

Brain tissue samples (middle frontal gyrus) from 41 cases of cognitively normal (CDR = 0 at death) participants were obtained from the Knight Alzheimer's Disease Research Center Neuropathology Core at Washington University. All brains were assessed using the neuropathologic criteria of the Consortium to Establish a Registry for Alzheimer's Disease (CERAD) and the NIA-Reagan Institute criteria for the neuropathologic diagnosis of AD (35, 57). The average age at death was 86.1 years (range 64.8–107.9 years). The post-mortem interval ranged from 2.3 to 24 h with a mean of 11.9 h. Age was not found to covary with apoE genotype in CSF, brain, or plasma studies, although age at death was significantly higher than older-cohort age at CSF collection by Student's t test (t(133) = 9.3, $p < 0.0001$). ApoE genotype and age ranges included brain, plasma, and CSF cases and are listed in Table 4.

Immunohistochemistry—All cases were assessed neuropathologically using an established protocol (58). Briefly, 6-μm sections were stained with hematoxylin and eosin (H&E) and cresyl violet. Immunohistochemistry was performed on deparaffinized and rehydrated sections. For β-amyloid immunohistochemistry, sections were pretreated with formic acid (98%) to enhance antigen retrieval. Sections were incubated with the following primary antibodies: anti-GFAP (1:1000; DAKO, Carpinteria, CA), mouse monoclonal anti-β-amyloid 10D5 (1:100,000; Lilly), and mouse monoclonal PHF-1 (1:500; a gift from Dr. Peter Davies, Albert Einstein College of Medicine,

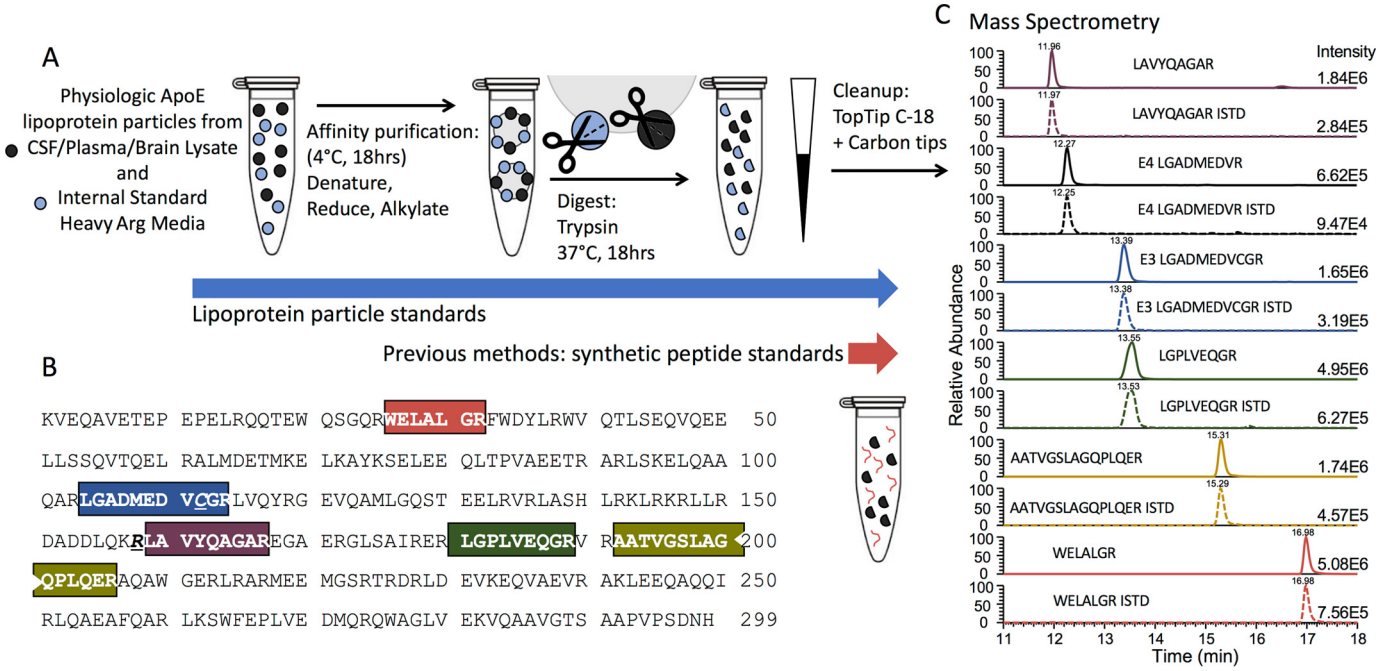

FIGURE 8. **ApoE sample preparation and peptide production for comparing apoE3 and apoE4 amounts.** *A*, apoE sample preparation. Similar molar amounts of target and molar-equilibrated ISTD apoE, in the form of physiologic lipoprotein particles, are combined in each sample and undergo purification and processing simultaneously. In contrast, previous methods introduce synthetic peptide standards at the end of the sample preparation process and immediately prior to MS analysis, not accounting for isoform bias that may affect the target apoE during immunoprecipitation, endoprotease digestion, or sample preparation. *B*, apoE3 sequence and tryptic peptides. Peptides selected for quantitation are *highlighted in boxes*, except apoE4 peptide. ApoE4 sequence substitutes arginine (R) at amino acid residue 112, resulting in isoform-specific tryptic peptide LGADMEDVR. Other peptides are common between apoE3 and apoE4 isoforms. *C*, LC/SRM mass spectrometry. Heavy arginine-labeled peptides (*dotted lines*) are eluted at the same retention time as unlabeled peptides (*solid lines*). All target peptides can be detected simultaneously in a sample, as demonstrated here with traces from *APOE*-ϵ3/ϵ4 subject CSF ith heavy arginine-labeled ISTD added.

New York). Species-specific biotinylated secondary antibodies were applied followed by avidin-horseradish peroxidase, and the chromogenic substrate diaminobenzidine tetrahydrochloride (Vector Laboratories, Burlingame, CA) was used for detection of horseradish peroxidase. To ensure even staining between sections, all sections were stained as a batch. Sections were counterstained with hematoxylin. Additional sections were set aside for quantitative densitometry and were not counterstained.

Estimation of β-Amyloid Plaque Burden—Stereologic counts of β-amyloid plaques were undertaken in sections of the frontal lobe (Brodmann's area 9) using the "area fraction fractionator" stereologic probe as implemented by the Stereo Investigator software package (MicroBrightField, Williston, VT) and a Nikon E800 microscope with motorized stage in three dimensions. Briefly, a two-dimensional counting probe (x and y dimensions of 50 × 50 μm) was applied to a systematic random sample of sites to include both the gyral crest and sulcal depth. The outline of the area of interest was outlined using a ×4 objective, and the β-amyloid plaque burden was determined using a ×20 lens.

Quantitative Immunohistochemistry of Diaminobenzidine Tetrahydrochloride-stained Sections—As we used several antibodies with optically continuous staining characteristics (variable grayscale intensities) and heterogeneous morphologic features, we employed computerized quantitative densitometric techniques as described previously (59). Quantitation of immunoreactive lesions on non-counterstained sections was undertaken by a single observer and performed as reported previously (59). Briefly, digital images were captured using a Nikon Eclipse 800 light microscope coupled to a XC30 digital camera (Olympus Imaging America, Center Valley, PA). All sections immunostained with one antibody were analyzed during a single session to minimize changes due to illumination, lamp intensity, or camera setting.

From each region of interest digital images representing three non-overlapping fields (0.09 mm^2) were captured. After each field was captured, the stage was moved manually to a new field using fiducial landmarks, as determined by differential interference contrast microscopy, to ensure non-redundant evaluation. Total immunoreactivity was estimated for each image by using the Set Threshold Function in the AnalySIS imaging software package (Olympus Soft Imaging Solutions, Lakewood, CO). Light intensity thresholds were selected to maximize the signal-to-noise ratio and were applied uniformly to all digital images. The Phase Analysis function reported the percentage of the entire field that was included within the threshold. This value is equivalent to the total percentage of immunoreactivity present per field.

Isolation of ApoE and Tryptic Digestion—ApoE purification and sample preparation are shown in Fig. 8*A*. ApoE was isolated from 0.1 ml of CSF, 0.35 ml of pooled E3* and E4* astrocyte media internal standard (described below), and 0.55 ml of PBS and processed as described previously (32). In brief, samples were incubated with PHM-LipoSorb (1:20 by volume, 18 h at 4 °C). The PHM-LipoSorb was prepared according to the manufacturer's instructions (1 g/50 ml of PBS). Adsorbed apoE was denatured and reduced in 40% trifluoroethanol, 100 mM triethylammonium bicarbonate, 5 mM dithiothreitol (DTT; 30 min,

37 °C). Samples were alkylated with 20 mM iodoacetamide (30 min at room temperature in the dark) and quenched with an additional 5 mM DTT (15 min at room temperature). Samples were diluted to 10% trifluoroethanol with 100 mM triethylammonium bicarbonate and then digested with trypsin (1.5 μg, 18 h, 37 °C; Sigma). Before analysis, samples were desalted using TopTip C-18 + carbon following the manufacturer's instructions (Glygen, Columbia, MD). After centrifugal evaporation (45 min at 37 °C), samples were resuspended in 30 μl of 5% acetonitrile, 0.1% formic acid. Brain apoE was prepared as described for CSF with the following modifications: apoE was isolated from samples containing 0.1 ml of 150 mg of tissue/ml of lysis buffer (containing 150 mM sodium chloride, 50 mM Tris-hydrochloride, 1% Triton X-100, and protease inhibitor, at pH 7.6) by immunoprecipitation with 5.5 mg/g Sepharose bead-conjugated WUE4 antibody, a monoclonal total apoE antibody (60). Prior to digest, apoE was eluted from beads with 100% formic acid and evaporated, and the pellet was washed with methanol. Plasma apoE was prepared as described for brain with the following exceptions: samples contained 0.02 ml of plasma, with internal standard and excess PBS to a 1-ml final volume. ELISA of pre- and post-purification apoE demonstrated pulldown efficacies of >99% for CSF by LipoSorb (5.7% coefficient of variations across three replicates) and >95% for brain by WUE4 (19.8% coefficient of variations across three replicates).

Trypsin digestion produced apoE isoform-specific peptides (inclusive of residue 112) LGADMEDVcGR ("c" indicates carboxamidomethyl cysteine residue methionine +57) from apoE3 and LGADMEDVR from apoE4, as well as four selected peptides distributed across the apoE sequence produced in common by both isoforms (WELALGR, LAVYQAGAR, LGPLVEQGR, and AATVGSLAGQPLQER; Fig. 8*B*). Samples were then analyzed on a Thermo Scientific TSQ Vantage mass spectrometer for selected reaction monitoring (SRM) analysis.

Production of Standards—ApoE3 and apoE4 isoform internal standards were obtained from the media of immortalized astrocytes derived from knock-in mice expressing human *APOE-ϵ3* or *APOE-ϵ4* (33). Astrocyte cultures were maintained in L-[U-$^{13}C_6$,$^{15}N_4$]arginine-enriched serum-free media to produce heavy arginine-labeled apoE media (E3* and E4* media). Label incorporation in apoE was 97% or higher. Unlabeled culture media were produced from the same cell lines (*E3* and *E4 media*; Fig. 1*A*). Heavy arginine media samples were cross-titrated with unlabeled media internal standards to establish the ratio at which a common peptide signal indicated an equivalent concentration between isoforms (Fig. 1, *B* and *C*). Multiple common peptides were assessed to avoid potential biases in detection between peptides. Each peptide provides a separate and independent assay supporting accurate and unbiased quantitation. This molar equivalent ratio of heavy arginine media was included in each sample as an internal standard.

An external standard curve was derived from separately pooled *APOE-ϵ3*/ϵ3 and *APOE-ϵ4*/ϵ4 CSF. These apoE3 and apoE4 CSF stocks were cross-equilibrated using the molar equivalent E3*/E4* media internal standard described above, and dilution curves of the apoE3/apoE4 molar-equilibrated CSF plus E3*/E4* media internal standard were used for normalization of peptide quantitation from CSF and brain samples.

Nano-LC Tandem MS and Quantitation—ApoE isoform-specific and common peptides were separated using reverse phase by a Waters nano-ACQUITY UPLC flowing at 500 nl/min through a nano-ACQUITY BEH 130 C18, 1.7-μm column (100 μm × 100 mm). Peptides were loaded at 4% solution B, followed by a three-stage gradient increasing to 12% B (over 3 min), to 35% B (7 min), and then to 95% B (3 min). The column was then washed for 2 min at 95% B and re-equilibrated for 2 min at 4% B (solution A = 0.1% formic acid, 2% DMSO in water, and solution B = 0.1% formic acid, 2% DMSO in acetonitrile).

Heavy arginine-labeled and -unlabeled peptides were detected by a TSQ Vantage mass spectrometer (Thermo Scientific, San Jose, CA) operating in SRM mode equipped with a nanospray ionization source (Phoenix S&T, Chester, PA). Optimized conditions were determined to be at a capillary temperature of 275 °C with a spray voltage of 1200 V and a collision gas pressure in Q2 of 2.0 mtorr. Peaks were detected and quantitated using Xcalibur 2.2 in batch processing mode and then reviewed and edited using Quan Browser (Thermo Scientific, San Jose, CA). Precursor and product ions for each monitored SRM transition are listed in Table 2 along with the associated instrument-dependent collision energies. Spectra with product ions for key apoE peptides used in the current analysis have been previously published (32). The SRM method monitored the doubly charged species of each peptide. All peptides were detected with abundant signal in a single LC/SRM run (Fig. 8*C*). The targeted isoform-specific peptides were consistent with the respective genotype of each individual.

ELISA—For human plasma (apoE3 + apoE4) ELISA, plates were coated with HJ15.6 (mouse monoclonal antibody generated in-house) at a concentration of 10 μg/ml in carbonate coating buffer at 4 °C overnight. After blocking with 2% BSA in PBS for 1 h at 37 °C, the samples were loaded on the plates and incubated overnight at 4 °C. Then the plates were incubated in 150 ng/ml HJ15.4-biotin (mouse monoclonal antibody generated in-house) for 1.5 h at 37 °C. Followed by an incubation in 1:10,000 streptavidin poly-HRP40 conjugate (Fitzgerald) for 1.5 h at room temperature, the plates were developed using Super Slow ELISA 3,3′,5,5′-tetramethylbenzidine (Sigma) and read on a Bio-Tek Synergy 2 plate reader at 650 nm. Recombinant apoE4 (Leinco) was used as the standard for human plasma apoE ELISA (61).

Efficiency of apoE purification comparing pre- and post-affinity-purified CSF (by PHM-LipoSorb, <99% recovery) and brain (by WUE4; 96% recovery) was assessed by sandwich ELISA using mouse monoclonal antibody HJ6.2 for capture and biotinylated HJ6.1 for detection. Both antibodies were generated in-house using astrocyte-derived mouse apoE as the antigen (39, 62). Recombinant human apoE3 (Leinco, St. Louis, MO) was used as a standard.

Statistical Analysis—ANOVA with Tukey's or linear trend tests post hoc and Student's *t* tests were carried out using GraphPad Prism software, version 6.05 (GraphPad Software, La Jolla, CA). Pearson's R correlation was calculated using Tableau Desktop Professional Edition, version 8.3 (Tableau Software Inc., Seattle, WA). Where apoE isoform measurements and comparisons were made across genotypes (between heterozygous and homozygous carriers of *APOE-ϵ3* or *APOE-ϵ4*), gene dose normal-

ization consisted of doubling the estimated isoform amount in heterozygote carriers. Isoform measures for homozygous participants and total apoE for all genotypes were not adjusted.

Author Contributions—A. T. B. N. conceived experiments, performed and analyzed experiments, and wrote the paper. K. G. M. designed and developed the LC-MS method and assisted in experimental design. J. G. B. edited the manuscript, provided feedback on interpretation of results, and contributed text in the Introduction and Discussion sections. V. O. assisted with experimental design, data analysis, and interpretation. T. K. assisted with assay and protocol design. F. L. performed and analyzed plasma ELISA for total apoE, with antibodies validated by H. J. D. H. provided feedback on experimental design. E. E. F. and N. J. C. performed immunohistochemical assays and provided pathology data for brain samples. J. C. M. provided the clinical characterizations of the older participants. R. J. B. conceived study design, obtained funding, assisted with experimental design, data analysis and interpretation, and manuscript writing and editing. All authors reviewed the results, provided feedback, and approved the final version of the paper.

Acknowledgments—We thank the research participants for their contributions in this study. We thank Nicholas Barthelemy, Rose Connors, Yaroslav Matviyiv, Sergio Molina, Chihiro Sato, Jason Ulrich, Michelle Wegscheid, and Hamideh Zakeri for their assistance in supporting the study, and the Clinical, Neuropathology, Genetics, Data Management and Biostatistics Cores of the Knight Alzheimer's Disease Research Center for participant assessments.

References

1. Mahley, R. W., and Rall, S. C. (2000) Apolipoprotein E: far more than a lipid transport protein. *Annu. Rev. Genomics Hum. Genet.* **1,** 507–537
2. Weisgraber, K. H., Rall, S. C., Jr., and Mahley, R. W. (1981) Human E apoprotein heterogeneity. Cysteine-arginine interchanges in the amino acid sequence of the apo-E isoforms. *J. Biol. Chem.* **256,** 9077–9083
3. Corder, E. H., Saunders, A. M., Risch, N. J., Strittmatter, W. J., Schmechel, D. E., Gaskell, P. C., Jr., Rimmler, J. B., Locke, P. A., Conneally, P. M., and Schmader, K. E. (1994) Protective effect of apolipoprotein-E type 2 allele for late onset Alzheimer disease. *Nat. Genet.* **7,** 180–184
4. Farrer, L. A., Cupples, L. A., Haines, J. L., Hyman, B., Kukull, W. A., Mayeux, R., Myers, R. H., Pericak-Vance, M. A., Risch, N., and van Duijn, C. M. (1997) Effects of age, sex, and ethnicity on the association between apolipoprotein E genotype and Alzheimer disease: a meta-analysis. *JAMA* **278,** 1349–1356
5. Ashford, J. W. (2004) APOE genotype effects on Alzheimer's disease onset and epidemiology. *J. Mol. Neurosci.* **23,** 157–165
6. Yu, J.-T., Tan, L., and Hardy, J. (2014) Apolipoprotein E in Alzheimer's disease: an update. *Annu. Rev. Neurosci.* **37,** 79–100
7. Namba, Y., Tomonaga, M., Kawasaki, H., Otomo, E., and Ikeda, K. (1991) Apolipoprotein E immunoreactivity in cerebral amyloid deposits and neurofibrillary tangles in Alzheimer's disease and kuru plaque amyloid in Creutzfeldt-Jakob disease. *Brain Res.* **541,** 163–166
8. Tokuda, T., Calero, M., Matsubara, E., Vidal, R., Kumar, A., Permanne, B., Zlokovic, B., Smith, J. D., Ladu, M. J., Rostagno, A., Frangione, B., and Ghiso, J. (2000) Lipidation of apolipoprotein E influences its isoform-specific interaction with Alzheimer's amyloid β peptides. *Biochem. J.* **348,** 359–365
9. Stratman, N. C., Castle, C. K., Taylor, B. M., Epps, D. E., Melchior, G. W., and Carter, D. B. (2005) Isoform-specific interactions of human apolipoprotein E to an intermediate conformation of human Alzheimer amyloid-β peptide. *Chem. Phys. Lipids.* **137,** 52–61
10. Strittmatter, W. J., Weisgraber, K. H., Huang, D. Y., Dong, L. M., Salvesen, G. S., Pericak-Vance, M., Schmechel, D., Saunders, A. M., Goldgaber, D., and Roses, A. D. (1993) Binding of human apolipoprotein E to synthetic amyloid β peptide: isoform-specific effects and implications for late-onset Alzheimer disease. *Proc. Natl. Acad. Sci. U.S.A.* **90,** 8098–8102
11. Belinson, H., Kariv-Inbal, Z., Kayed, R., Masliah, E., and Michaelson, D. M. (2010) Following activation of the amyloid cascade, apolipoprotein E4 drives the *in vivo* oligomerization of amyloid-β resulting in neurodegeneration. *J. Alzheimers Dis.* **22,** 959–970
12. Schmechel, D. E., Saunders, A. M., Strittmatter, W. J., Crain, B. J., Hulette, C. M., Joo, S. H., Pericak-Vance, M. A., Goldgaber, D., and Roses, A. D. (1993) Increased amyloid β-peptide deposition in cerebral cortex as a consequence of apolipoprotein E genotype in late-onset Alzheimer disease. *Proc. Natl. Acad. Sci. U.S.A.* **90,** 9649–9653
13. Christensen, D. Z., Schneider-Axmann, T., Lucassen, P. J., Bayer, T. A., and Wirths, O. (2010) Accumulation of intraneuronal Aβ correlates with apoE4 genotype. *Acta Neuropathol.* **119,** 555–566
14. Zerbinatti, C. V., Wahrle, S. E., Kim, H., Cam, J. A., Bales, K., Paul, S. M., Holtzman, D. M., and Bu, G. (2006) Apolipoprotein E and low density lipoprotein receptor-related protein facilitate intraneuronal Aβ42 accumulation in amyloid model mice. *J. Biol. Chem.* **281,** 36180–36186
15. Zhao, W., Dumanis, S. B., Tamboli, I. Y., Rodriguez, G. A., Jo Ladu, M., Moussa, C. E., and William Rebeck, G. (2014) Human APOE genotype affects intraneuronal Aβ1–42 accumulation in a lentiviral gene transfer model. *Hum. Mol. Genet.* **23,** 1365–1375
16. Castellano, J. M., Kim, J., Stewart, F. R., Jiang, H., DeMattos, R. B., Patterson, B. W., Fagan, A. M., Morris, J. C., Mawuenyega, K. G., Cruchaga, C., Goate, A. M., Bales, K. R., Paul, S. M., Bateman, R. J., and Holtzman, D. M. (2011) Human apoE isoforms differentially regulate brain amyloid-β peptide clearance. *Sci. Transl. Med.* **3,** 89ra57
17. Kang, D. E., Pietrzik, C. U., Baum, L., Chevallier, N., Merriam, D. E., Kounnas, M. Z., Wagner, S. L., Troncoso, J. C., Kawas, C. H., Katzman, R., and Koo, E. H. (2000) Modulation of amyloid β-protein clearance and Alzheimer's disease susceptibility by the LDL receptor–related protein pathway. *J. Clin. Invest.* **106,** 1159–1166
18. Bell, R. D., Sagare, A. P., Friedman, A. E., Bedi, G. S., Holtzman, D. M., Deane, R., and Zlokovic, B. V. (2007) Transport pathways for clearance of human Alzheimer's amyloid β-peptide and apolipoproteins E and J in the mouse central nervous system. *J. Cereb. Blood Flow Metab.* **27,** 909–918
19. Dorey, E., Chang, N., Liu, Q. Y., Yang, Z., and Zhang, W. (2014) Apolipoprotein E, amyloid-β, and neuroinflammation in Alzheimer's disease. *Neurosci. Bull.* **30,** 317–330
20. Mahley, R. W., and Huang, Y. (2012) Apolipoprotein E sets the stage: response to injury triggers neuropathology. *Neuron* **76,** 871–885
21. Brecht, W. J., Harris, F. M., Chang, S., Tesseur, I., Yu, G.-Q., Xu, Q., Dee Fish, J., Wyss-Coray, T., Buttini, M., Mucke, L., Mahley, R. W., and Huang, Y. (2004) Neuron-specific apolipoprotein E4 proteolysis is associated with increased tau phosphorylation in brains of transgenic mice. *J. Neurosci.* **24,** 2527–2534
22. Linton, M. F., Gish, R., Hubl, S. T., Bütler, E., Esquivel, C., Bry, W. I., Boyles, J. K., Wardell, M. R., and Young, S. G. (1991) Phenotypes of apolipoprotein B and apolipoprotein E after liver transplantation. *J. Clin. Invest.* **88,** 270–281
23. Panza, F., Solfrizzi, V., Colacicco, A. M., Basile, A. M., D'Introno, A., Capurso, C., Sabba, M., Capurso, S., and Capurso, A. (2003) Apolipoprotein E (APOE) polymorphism influences serum APOE levels in Alzheimer's disease patients and centenarians. *NeuroReport.* **14,** 605–608
24. Cruchaga, C., Kauwe, J. S., Nowotny, P., Bales, K., Pickering, E. H., Mayo, K., Bertelsen, S., Hinrichs, A., Alzheimer's Disease Neuroimaging Initiative, Fagan, A. M., Holtzman, D. M., Morris, J. C., and Goate, A. M. (2012) Cerebrospinal fluid APOE levels: an endophenotype for genetic studies for Alzheimer's disease. *Hum. Mol. Genet.* **21,** 4558–4571
25. Martínez-Morillo, E., Hansson, O., Atagi, Y., Bu, G., Minthon, L., Diamandis, E. P., and Nielsen, H. M. (2014) Total apolipoprotein E levels and specific isoform composition in cerebrospinal fluid and plasma from Alzheimer's disease patients and controls. *Acta Neuropathol.* **127,** 633–643
26. Simon, R., Girod, M., Fonbonne, C., Salvador, A., Clément, Y., Lantéri, P., Amouyel, P., Lambert, J. C., and Lemoine, J. (2012) Total apoE and apoE4 isoform assays in an Alzheimer's disease case-control study by targeted mass spectrometry (n=669): a pilot assay for methionine-containing proteotypic peptides. *Mol. Cell. Proteomics* **11,** 1389–1403
27. Fukumoto, H., Ingelsson, M., Gårevik, N., Wahlund, L. O., Nukina, N., Yaguchi, Y., Shibata, M., Hyman, B. T., Rebeck, G. W., and Irizarry, M. C.

(2003) APOE ϵ3/ϵ4 heterozygotes have an elevated proportion of apolipoprotein E4 in cerebrospinal fluid relative to plasma, independent of Alzheimer's disease diagnosis. *Exp. Neurol.* **183,** 249–253
28. Wahrle, S. E., and Holtzman, D. M. (2003) Differential metabolism of apoE isoforms in plasma and CSF. *Exp. Neurol.* **183,** 4–6
29. Fryer, J. D., Simmons, K., Parsadanian, M., Bales, K. R., Paul, S. M., Sullivan, P. M., and Holtzman, D. M. (2005) Human apolipoprotein E4 alters the amyloid-β 40:42 ratio and promotes the formation of cerebral amyloid angiopathy in an amyloid precursor protein transgenic model. *J. Neurosci.* **25,** 2803–2810
30. Aebersold, R., and Mann, M. (2003) Mass spectrometry-based proteomics. *Nature* **422,** 198–207
31. Martínez-Morillo, E., Nielsen, H. M., Batruch, I., Drabovich, A. P., Begcevic, I., Lopez, M. F., Minthon, L., Bu, G., Mattsson, N., Portelius, E., Hansson, O., and Diamandis, E. P. (2014) Assessment of peptide chemical modifications on the development of an accurate and precise multiplex selected reaction monitoring assay for apolipoprotein E isoforms. *J. Proteome Res.* **13,** 1077–1087
32. Wildsmith, K. R., Han, B., and Bateman, R. J. (2009) Method for the simultaneous quantitation of apolipoprotein E isoforms using tandem mass spectrometry. *Anal. Biochem.* **395,** 116–118
33. Morikawa, M., Fryer, J. D., Sullivan, P. M., Christopher, E. A., Wahrle, S. E., DeMattos, R. B., O'Dell, M. A., Fagan, A. M., Lashuel, H. A., Walz, T., Asai, K., and Holtzman, D. M. (2005) Production and characterization of astrocyte-derived human apolipoprotein E isoforms from immortalized astrocytes and their interactions with amyloid-β. *Neurobiol. Dis.* **19,** 66–76
34. Braak, H., and Braak, E. (1995) Staging of Alzheimer's disease-related neurofibrillary changes. *Neurobiol. Aging* **16,** 271–278
35. Mirra, S. S., Heyman, A., McKeel, D., Sumi, S. M., Crain, B. J., Brownlee, L. M., Vogel, F. S., Hughes, J. P., van Belle, G., and Berg, L. (1991) The consortium to establish a registry for Alzheimer's disease (CERAD). Part II. standardization of the neuropathologic assessment of Alzheimer's disease. *Neurology* **41,** 479–486
36. Thal, D. R., Rüb, U., Orantes, M., and Braak, H. (2002) Phases of Aβ-deposition in the human brain and its relevance for the development of AD. *Neurology* **58,** 1791–1800
37. DeMattos, R. B., Bales, K. R., Cummins, D. J., Dodart, J.-C., Paul, S. M., and Holtzman, D. M. (2001) Peripheral anti-Aβ antibody alters CNS and plasma Aβ clearance and decreases brain Aβ burden in a mouse model of Alzheimer's disease. *Proc. Natl. Acad. Sci. U.S.A.* **98,** 8850–8855
38. Hoofnagle, A. N., and Wener, M. H. (2009) The fundamental flaws of immunoassays and potential solutions using tandem mass spectrometry. *J. Immunol. Methods* **347,** 3–11
39. Verghese, P. B., Castellano, J. M., Garai, K., Wang, Y., Jiang, H., Shah, A., Bu, G., Frieden, C., and Holtzman, D. M. (2013) ApoE influences amyloid-β (Aβ) clearance despite minimal apoE/Aβ association in physiological conditions. *Proc. Natl. Acad. Sci. U.S.A.* **110,** E1807–E1816
40. Morris, J. C., Roe, C. M., Xiong, C., Fagan, A. M., Goate, A. M., Holtzman, D. M., and Mintun, M. A. (2010) APOE predicts amyloid-beta but not tau Alzheimer pathology in cognitively normal aging. *Ann. Neurol.* **67,** 122–131
41. Riddell, D. R., Zhou, H., Atchison, K., Warwick, H. K., Atkinson, P. J., Jefferson, J., Xu, L., Aschmies, S., Kirksey, Y., Hu, Y., Wagner, E., Parratt, A., Xu, J., Li, Z., Zaleska, M. M., *et al.* (2008) Impact of apolipoprotein E (apoE) polymorphism on brain apoE levels. *J. Neurosci.* **28,** 11445–11453
42. Fukuyama, R., Mizuno, T., Mori, S., Yanagisawa, K., Nakajima, K., and Fushiki, S. (2000) Age-dependent decline in the apolipoprotein E level in cerebrospinal fluid from control subjects and its increase in cerebrospinal fluid from patients with Alzheimer's disease. *Eur. Neurol.* **43,** 161–169
43. Toledo, J. B., Da, X., Weiner, M. W., Wolk, D. A., Xie, S. X., Arnold, S. E., Davatzikos, C., Shaw, L. M., Trojanowski, J. Q., Alzheimer's Disease Neuroimaging Initiative. (2014) CSF apo-E levels associate with cognitive decline and MRI changes. *Acta Neuropathol.* **127,** 621–632
44. Gregg, R. E., Zech, L. A., Schaefer, E. J., Stark, D., Wilson, D., and Brewer, H. B. (1986) Abnormal *in vivo* metabolism of apolipoprotein E4 in humans. *J. Clin. Invest.* **78,** 815–821
45. Kadish, I., Thibault, O., Blalock, E. M., Chen, K.-C., Gant, J. C., Porter, N. M., and Landfield, P. W. (2009) Hippocampal and cognitive aging across the life span: a bioenergetic shift precedes and increased cholesterol trafficking parallels memory impairment. *J. Neurosci.* **29,** 1805–1816
46. Middeldorp, J., and Hol, E. M. (2011) GFAP in health and disease. *Prog. Neurobiol.* **93,** 421–443
47. Pitas, R. E., Boyles, J. K., Lee, S. H., Foss, D., and Mahley, R. W. (1987) Astrocytes synthesize apolipoprotein E and metabolize apolipoprotein E-containing lipoproteins. *Biochim. Biophys. Acta* **917,** 148–161
48. Blalock, E. M., Chen, K.-C., Sharrow, K., Herman, J. P., Porter, N. M., Foster, T. C., and Landfield, P. W. (2003) Gene microarrays in hippocampal aging: statistical profiling identifies novel processes correlated with cognitive impairment. *J. Neurosci.* **23,** 3807–3819
49. Steinmetz, A., Jakobs, C., Motzny, S., and Kaffarnik, H. (1989) Differential distribution of apolipoprotein E isoforms in human plasma lipoproteins. *Arteriosclerosis* **9,** 405–411
50. Weisgraber, K. H. (1990) Apolipoprotein E distribution among human plasma lipoproteins: role of the cysteine-arginine interchange at residue 112. *J. Lipid Res.* **31,** 1503–1511
51. Oikawa, N., Hatsuta, H., Murayama, S., Suzuki, A., and Yanagisawa, K. (2014) Influence of APOE genotype and the presence of Alzheimer's pathology on synaptic membrane lipids of human brains. *J. Neurosci. Res.* **92,** 641–650
52. Jiang, Q., Lee, C. Y., Mandrekar, S., Wilkinson, B., Cramer, P., Zelcer, N., Mann, K., Lamb, B., Willson, T. M., Collins, J. L., Richardson, J. C., Smith, J. D., Comery, T. A., Riddell, D., Holtzman, D. M., Tontonoz, P., and Landreth, G. E. (2008) apoE promotes the proteolytic degradation of Aβ. *Neuron* **58,** 681–693
53. Bateman, R. J., Munsell, L. Y., Morris, J. C., Swarm, R., Yarasheski, K. E., and Holtzman, D. M. (2006) Human amyloid-β synthesis and clearance rates as measured in cerebrospinal fluid *in vivo*. *Nat. Med.* **12,** 856–861
54. Huang, Y., Potter, R., Sigurdson, W., Santacruz, A., Shih, S., Ju, Y.-E., Kasten, T., Morris, J. C., Mintun, M., Duntley, S., and Bateman, R. J. (2012) Effects of age and amyloid deposition on Aβ dynamics in the human central nervous system. *Arch. Neurol.* **69,** 51–58
55. Potter, R., Patterson, B. W., Elbert, D. L., Ovod, V., Kasten, T., Sigurdson, W., Mawuenyega, K., Blazey, T., Goate, A., Chott, R., Yarasheski, K. E., Holtzman, D. M., Morris, J. C., Benzinger, T. L., and Bateman, R. J. (2013) Increased *in vivo* amyloid-β42 production, exchange, and loss in presenilin mutation carriers. *Sci. Transl. Med.* **5,** 189ra77
56. Mintun, M. A., Larossa, G. N., Sheline, Y. I., Dence, C. S., Lee, S. Y., Mach, R. H., Klunk, W. E., Mathis, C. A., DeKosky, S. T., and Morris, J. C. (2006) [^{11}C]PIB in a nondemented population: potential antecedent marker of Alzheimer disease. *Neurology* **67,** 446–452
57. Hyman, B. T., Phelps, C. H., Beach, T. G., Bigio, E. H., Cairns, N. J., Carrillo, M. C., Dickson, D. W., Duyckaerts, C., Frosch, M. P., Masliah, E., Mirra, S. S., Nelson, P. T., Schneider, J. A., Thal, D. R., Thies, B., Trojanowski, J. Q., Vinters, H. V., and Montine, T. J. (2012) National Institute on Aging–Alzheimer's Association guidelines for the neuropathologic assessment of Alzheimer's disease. *Alzheimers Dement.* **8,** 1–13
58. Cairns, N. J., Taylor-Reinwald, L., Morris, J. C., Alzheimer's Disease Neuroimaging Initiative. (2010) Autopsy consent, brain collection, and standardized neuropathologic assessment of ADNI participants: the essential role of the neuropathology core. *Alzheimers Dement.* **6,** 274–279
59. Ghoshal, N., Dearborn, J. T., Wozniak, D. F., and Cairns, N. J. (2012) Core features of frontotemporal dementia recapitulated in progranulin knockout mice. *Neurobiol. Dis.* **45,** 395–408
60. Krul, E. S., Tikkanen, M. J., and Schonfeld, G. (1988) Heterogeneity of apolipoprotein E epitope expression on human lipoproteins: importance for apolipoprotein E function. *J. Lipid Res.* **29,** 1309–1325
61. Liao, F., Zhang, T. J., Jiang, H., Lefton, K. B., Robinson, G. O., Vassar, R., Sullivan, P. M., and Holtzman, D. M. (2015) Murine *versus* human apolipoprotein E4: differential facilitation of and co-localization in cerebral amyloid angiopathy and amyloid plaques in APP transgenic mouse models. *Acta Neuropathol. Commun.* **3,** 70
62. Basak, J. M., Verghese, P. B., Yoon, H., Kim, J., and Holtzman, D. M. (2012) Low-density lipoprotein receptor represents an apolipoprotein E-independent pathway of Aβ uptake and degradation by astrocytes. *J. Biol. Chem.* **287,** 13959–13971

Human Central Nervous System (CNS) ApoE Isoforms Are Increased by Age, Differentially Altered by Amyloidosis, and Relative Amounts Reversed in the CNS Compared with Plasma

Alaina T. Baker-Nigh, Kwasi G. Mawuenyega, James G. Bollinger, Vitaliy Ovod, Tom Kasten, Erin E. Franklin, Fan Liao, Hong Jiang, David Holtzman, Nigel J. Cairns, John C. Morris and Randall J. Bateman

J. Biol. Chem. 2016, 291:27204-27218.
doi: 10.1074/jbc.M116.721779 originally published online October 28, 2016
